Electronic Supplementary Material (ESI) for Journal of Materials Chemistry C.

Artificial Light-Harvesting System with Sequential Energy Transfer for Information Dual Encryption and Anticounterfeiting

Yan Xia,[†] Maowen Chen,[†] Suwan Li,[†] Man Li,[†] Xianying Li,[‡] Tao Yi,[†]* and Dengqing Zhang[†]*

[†] College of Chemistry, Chemical Engineering and Biotechnology, Donghua University, Shanghai, 201620, China

[‡] School of Environmental Science and Engineering, Donghua University, Shanghai, 201620, China

Table of contents

1. General information

All reagents and solvents were commercially available and used without further purification. The compounds **L1**[1], **L2**[2] and **1**[3] were prepared according to the published procedures. ^{1}H NMR and ^{13}C NMR spectra were recorded in $CDCl_3$ or DMSO-d_6 on Bruker Model Avance DMX 400 (400 MHz). Absorption spectra were recorded on a PERSEE model TU-1901 spectrophotometer. Fluorescence spectra were recorded on a F-7000 FL Spectrophotometer. The fluorescence lifetimes were measured employing time correlated single photon counting on a FLS980 instrument. The fluorescence quantum yields were measured on a PTI QM 40 instrument with the integrating sphere. Transmission electron microscopy (TEM) images were carried out on a JEOL JEM-2100 instrument. Scanning electron microscopy (SEM) images were recorded with a Hitachi S-4800 or SU8010 instruments. Dynamic light scattering (DLS) measurements were performed at a Malvern Instrument. Zeta-potential measurements were performed on a Zetasizer Nano Z apparatus at 25 ℃. ESI-TOF-mass spectrum was recorded on a Micromass Quattro II triple-quadrupole mass spectrometer using electrospray ionization with a MassLynx operating system.

2. Synthesis of MPy1

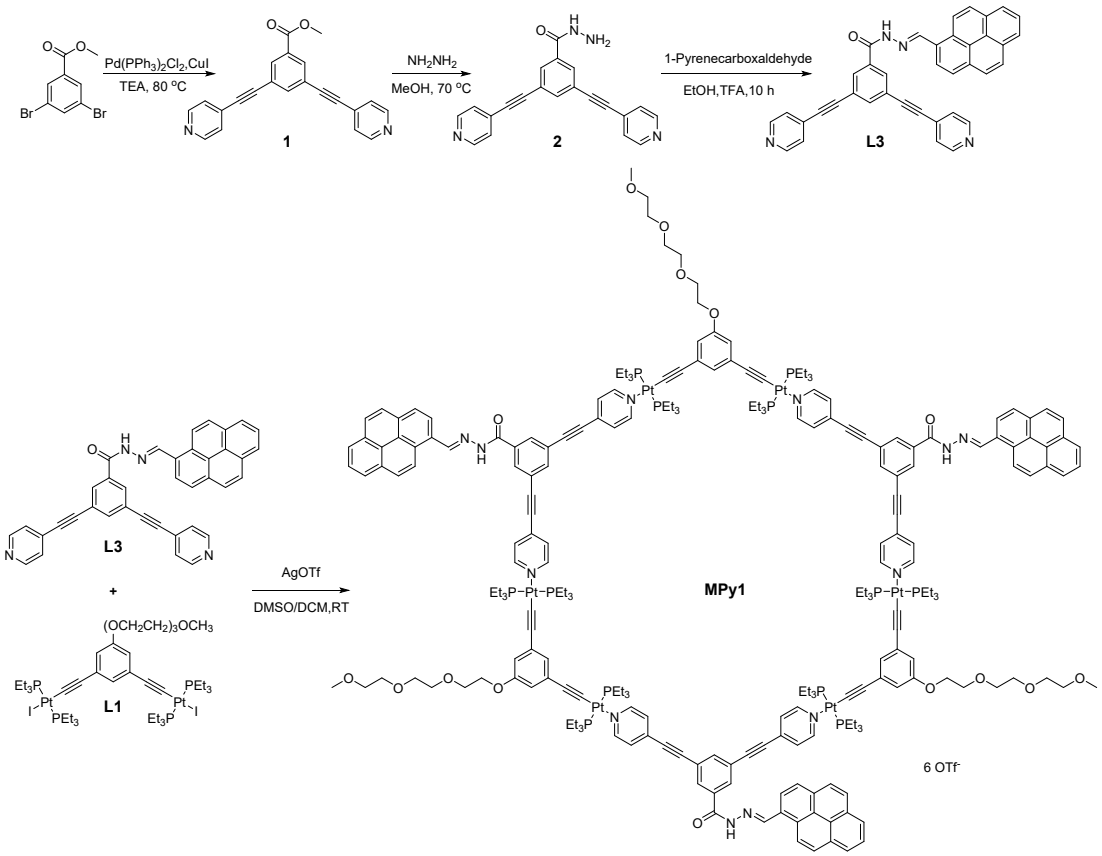

Figure S1. Synthesis route of **MPy1**.

Synthesis of **1**[3]

In a dry Schlenk tube, $Pd(PPh_3)Cl_2$ (140 mg, 0.2 mmol, 0.1 eq) was solubilized in freshly distilled and degassed triethylamine (13 mL) at 80 °C. Methyl 3,5-dibromobenzoate (250 mg, 0.85 mmol), 3-ethynylpyridine (263 mg, 2.55 mmol) and CuI (32.4 mg, 0.17 mmol) were successively added, and the resulting mixture was heated to 80 °C under argon overnight. The solvent was removed in vacuo and the crude brown powder was purified by column chromatography on silica gel (PE: EA = 1:1) to give white solid (88 mg, 65 %). ^{1}H NMR (400 MHz, $CDCl_3$) δ 8.65 (d, J = 3.2 Hz, 4H), 8.23 (d, J = 1.4 Hz, 2H), 7.92 (d, J = 1.4 Hz, 1H), 7.42 (d, J = 5.6 Hz, 4H), 3.98 (s, 3H).

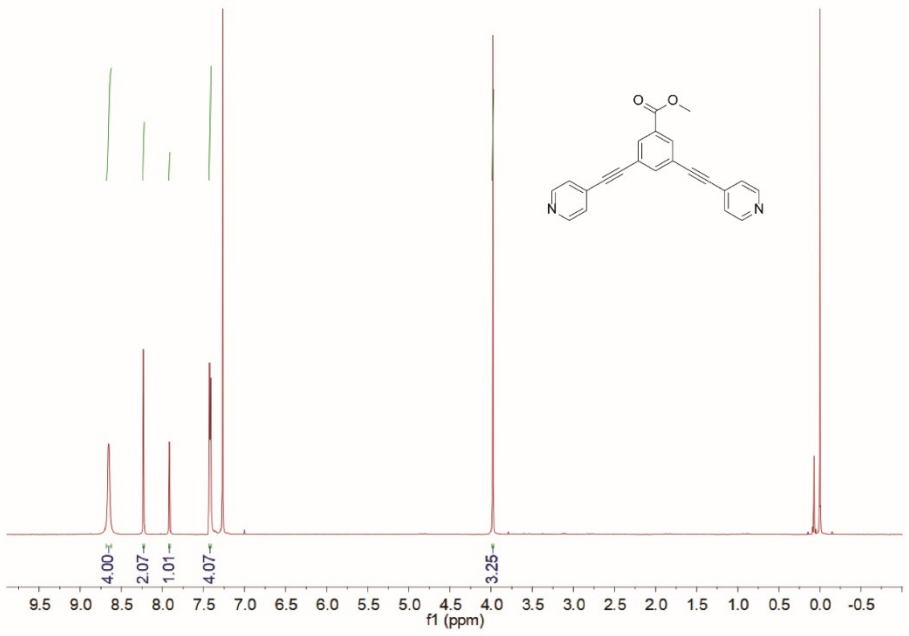

Figure S2. ^{1}H NMR spectrum (400 MHz, $CDCl_3$, 298K) of compound **1**.

Synthesis of 2

Compound **1** (120 mg, 0.3546 mmol, 1 eq), hydrazine monohydrate (1 mL) and MeOH (10 mL) were mixed together and refluxed for 12 h at 70 °C under inert atmosphere. Then reaction was stopped and cooled to room temperature and methanol was evaporated. The product was extracted with dichloromethane (30 mL) and washed with water (3×50 mL) and brine solution (20 mL). The organic layer was dried over anhydrous Na_2SO_4 and solvent was evaporated to get the crude product as light brown oil (400 mg, 80 %). ^{1}H NMR (400 MHz, DMSO-d_6) δ 10.02 (s, 1H), 8.68 (d, *J*=4.9Hz, 4H), 8.12 (s, 2H), 8.01 (s, 1H), 7.58 (d, *J*=4.9Hz, 4H). ^{13}C NMR (101 MHz, DMSO-d_6) δ 164.22, 150.48, 137.12, 134.94, 131.38, 130.11, 125.95, 122.77, 92.00, 88.48. ESI-MS: m/z Calcd for $C_{21}H_{14}N_4O$ $[M+H]^+$ 339.1, found 339.1.

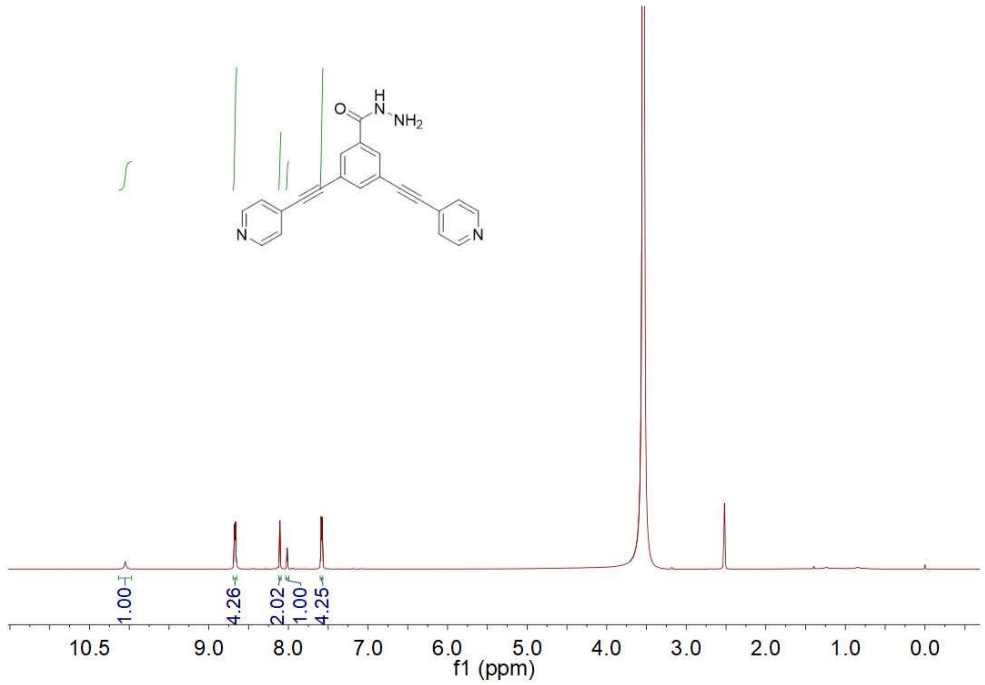

Figure S3. ^{1}H NMR spectrum of **2** in DMSO-d_6.

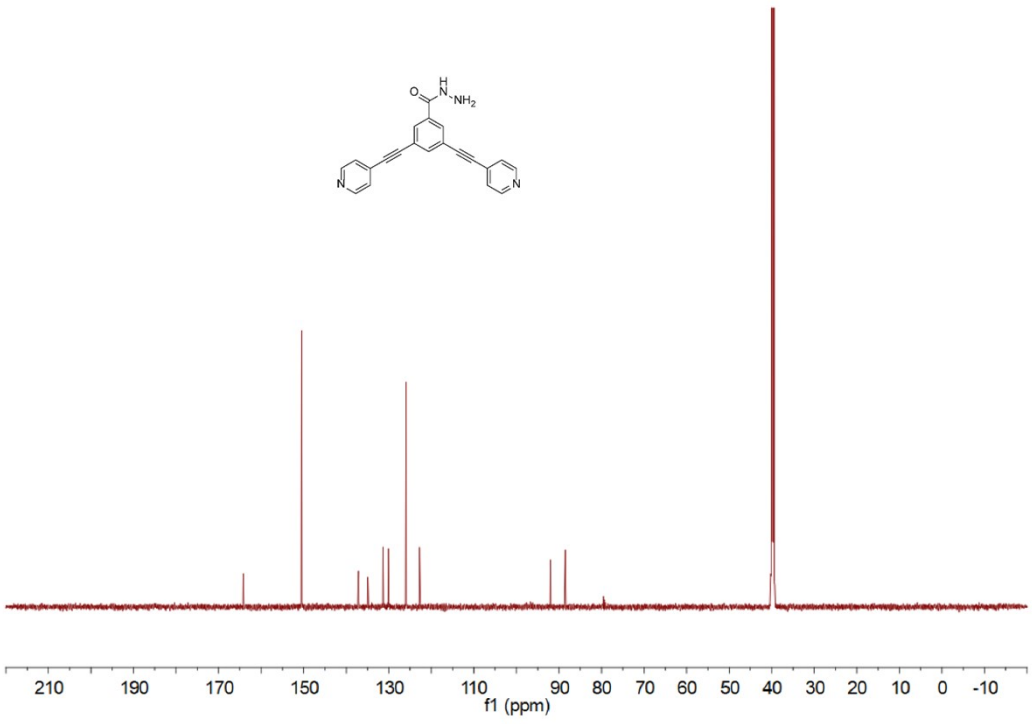

Figure S4. ^{13}C NMR spectrum of **2** in DMSO-d_6.

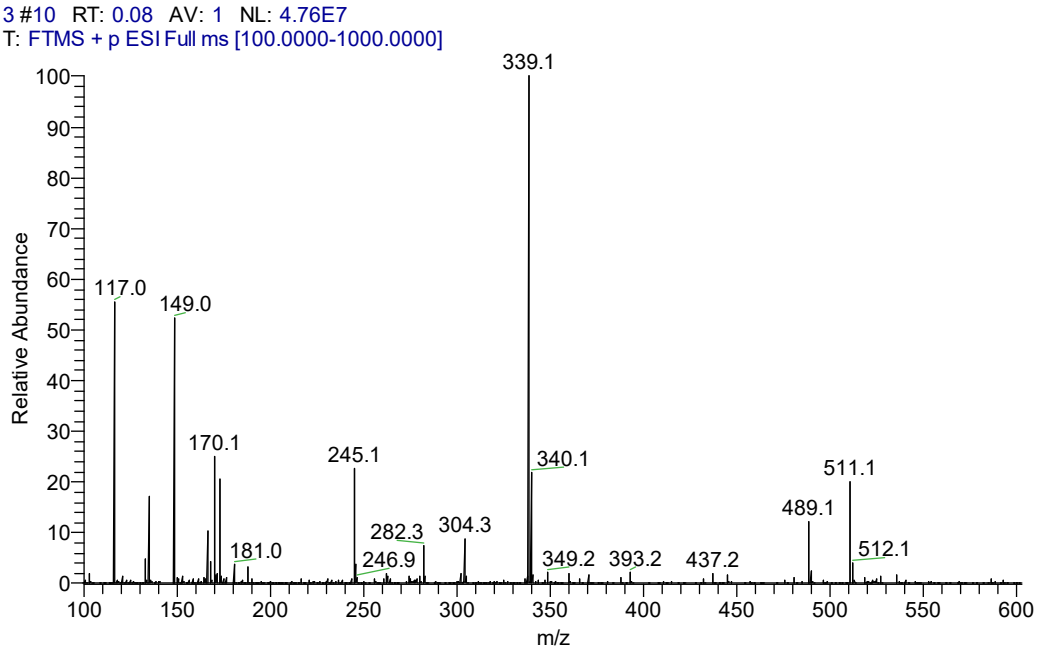

Figure S5. ESI spectrum of compound **2**.

Synthesis of L3

To an ethanol solution of **2** (0.4064 mmol, 137 mg in 5 mL dry ethanol) was added a solution of 1-pyrenecarboxaldehyde (0.4064 mmol, 100 mg in 10 mL ethanol). The reaction mixture was stirred for 16 h. Then the mixture was allowed to cool to room temperature to produce a yellow precipitate. The crude product was purified by recrystallization with ethanol to afford compound **L3** as a yellow-green solid (160 mg). Yield: 64.8%. ^{1}H NMR (400 MHz, DMSO-d_6) δ 12.28 (s, 1H), 9.56 (s, 1H), 8.84 (d, J = 9.3 Hz, 1H), 8.72 (d, J = 4.4 Hz, 4H), 8.62 (d, J = 7.9 Hz, 1H), 8.41 (d, J = 7.2 Hz, 4H), 8.34 – 8.25 (m, 4H), 8.16 (s, 2H), 7.65 (d, J = 4.7 Hz, 4H). ^{13}C NMR (101 MHz, DMSO-d_6) δ 164.05, 150.09, 138.55, 136.87, 131.66, 131.22, 130.94, 130.42, 129.68, 127.83, 127.70, 127.60, 126.97, 126.09, 125.91, 125.71, 125.51, 125.40, 124.83, 124.23, 123.40, 123.20, 86.30, 80.10. ESI-MS: m/z Calcd for $C_{38}H_{22}N_4O$ $[M+H]^+$ 551.2, found 551.2.

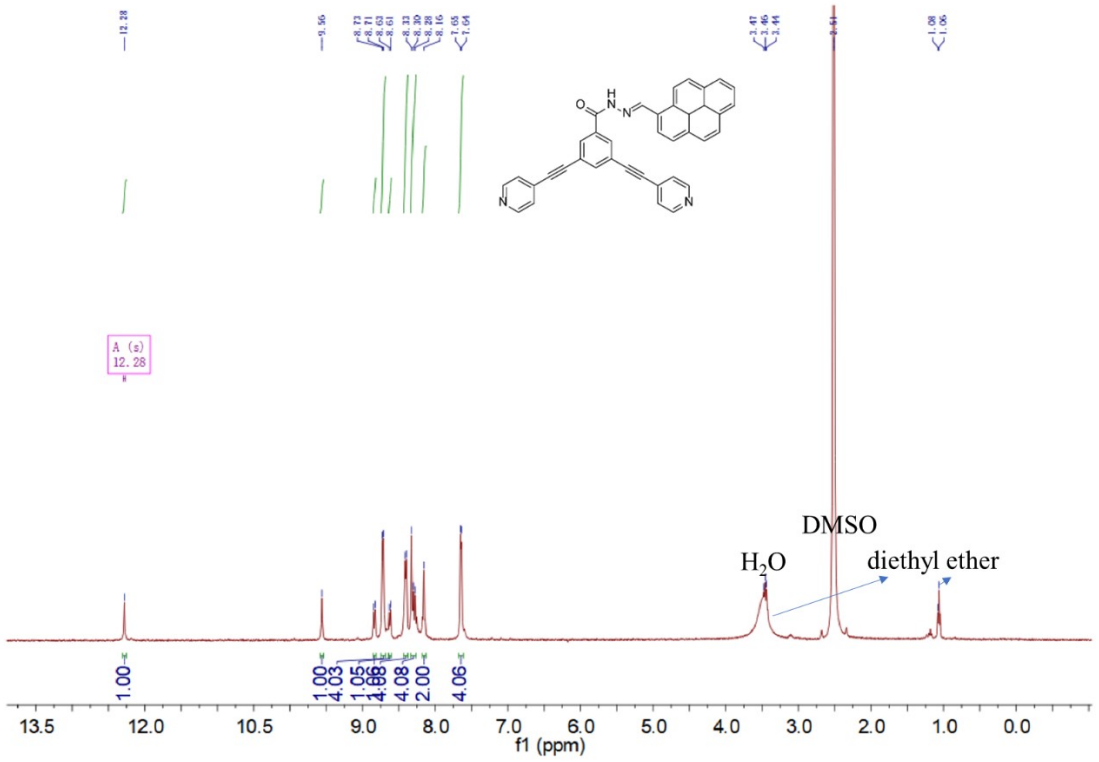

Figure S6. ^{1}H NMR spectrum of **L3** in DMSO-d_6.

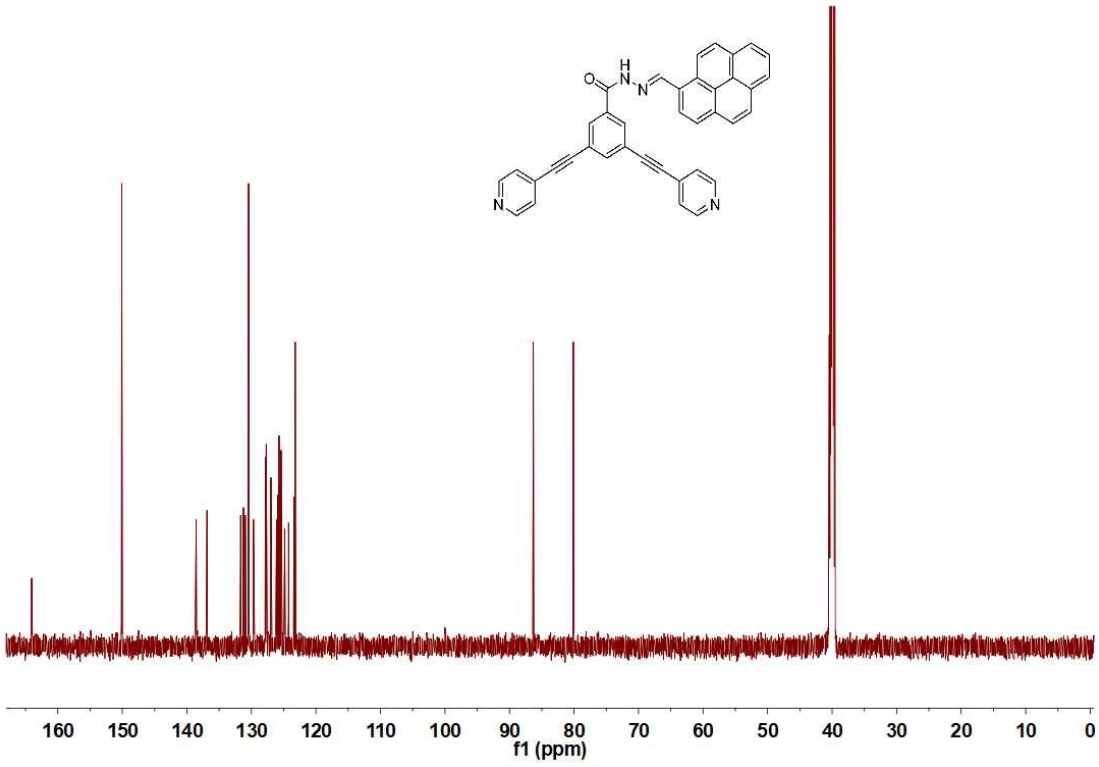

Figure S7. ^{13}C NMR spectrum of **L3** in DMSO-d_6 at 323 K.

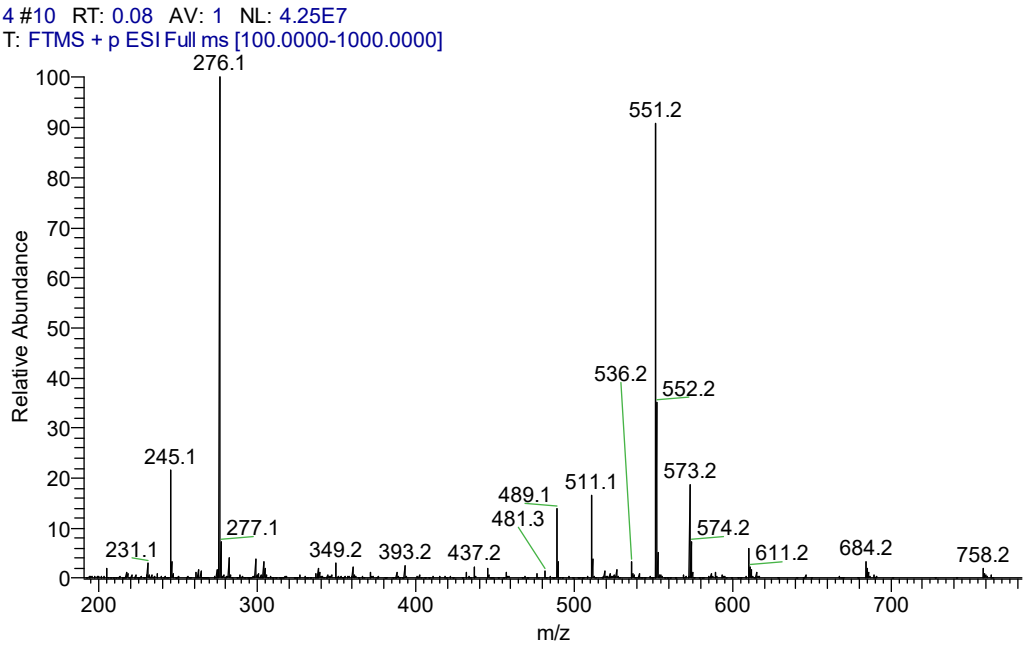

Figure S8. ESI spectrum of compound **L3.**

Synthesis of MPy1

L1 (10 mg, 7.0 μmol), AgOTf (5.5 mg, 21.0 μmol) and **L3** (4 mg, 7.0 μmol) were dissolved in the mixture of DMSO and DCM (2.0 mL, V_{DCM}:V_{DMSO} = 10:1) in a 20 mL glass vial. The reaction mixture was allowed to stir for 6 h at room temperature, and the reaction mixture was centrifuged at 3400 r/h for 20 min. To the resulting homogeneous solution, diethyl ether was added to precipitate the product, which was then isolated and dried under reduced pressure and re-dissolved in DMSO-d_6 for characterization. ^{1}H NMR (400 MHz, DMSO-d_6) δ 12.30 (s, 1H), 9.54 (s, 1H), 8.95 – 8.82 (m, 5H), 8.61 (d, J = 8.7 Hz, 1H), 8.41 (d, J = 9.4 Hz, 4H), 8.34 – 8.15 (m, 6H), 7.91 (s, 4H), 6.64 (s, 2H), 6.53 (s, d, J = 22.3 Hz, 1H), 4.08 (d, J = 5.8 Hz, 2H), 3.73 (s, 2H), 3.60 – 3.50 (m, 6H), 3.44 – 3.42 (m, 2H), 3.25 (s, 3H), 1.82 (s, 24H), 1.19 – 1.06 (m, 36H). ^{31}P NMR (121.4 MHz, DMSO-d_6) δ (ppm) 15.52 (s, ^{195}Pt satellites, $^1J_{Pt\text{-}P}$ = 1729.95 Hz). ESI-TOF-MS: $C_{243}H_{300}F_{18}N_{12}O_{33}P_{12}Pt_6S_6$ m/z [**M**-3OTf]$^{3+}$ 1849.39; [**M**-4OTf]$^{4+}$ 1348.28.

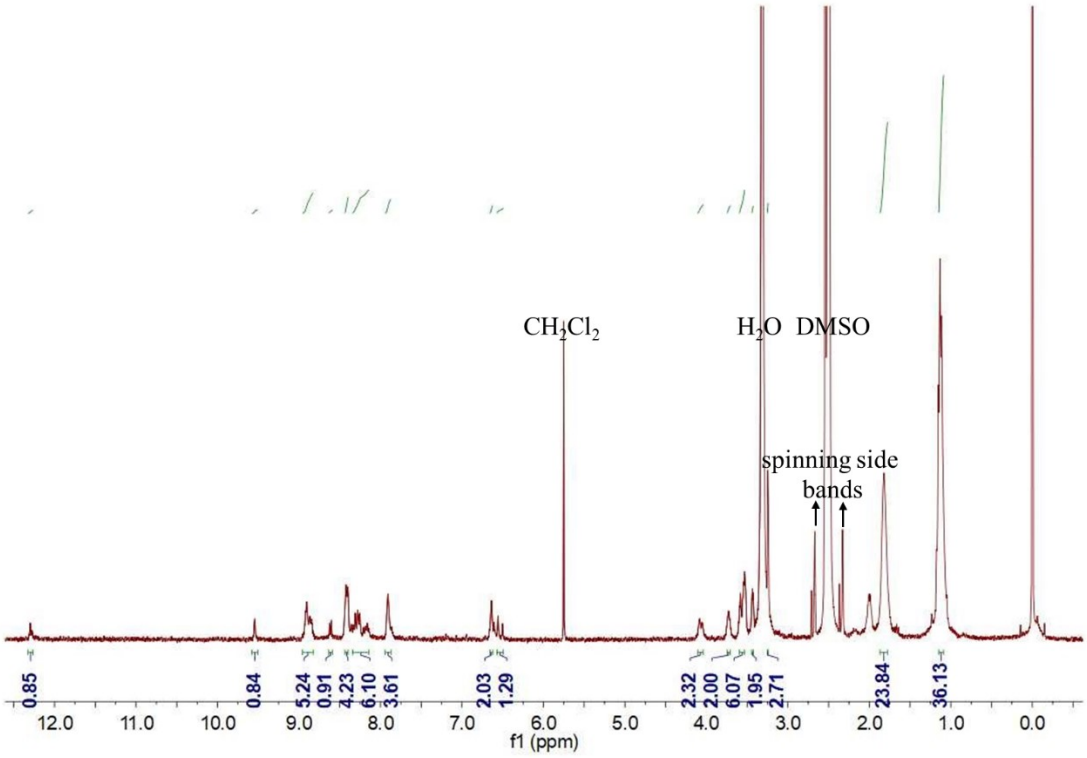

Figure S9. ^{1}H NMR spectrum of **MPy1** in DMSO-d_6.

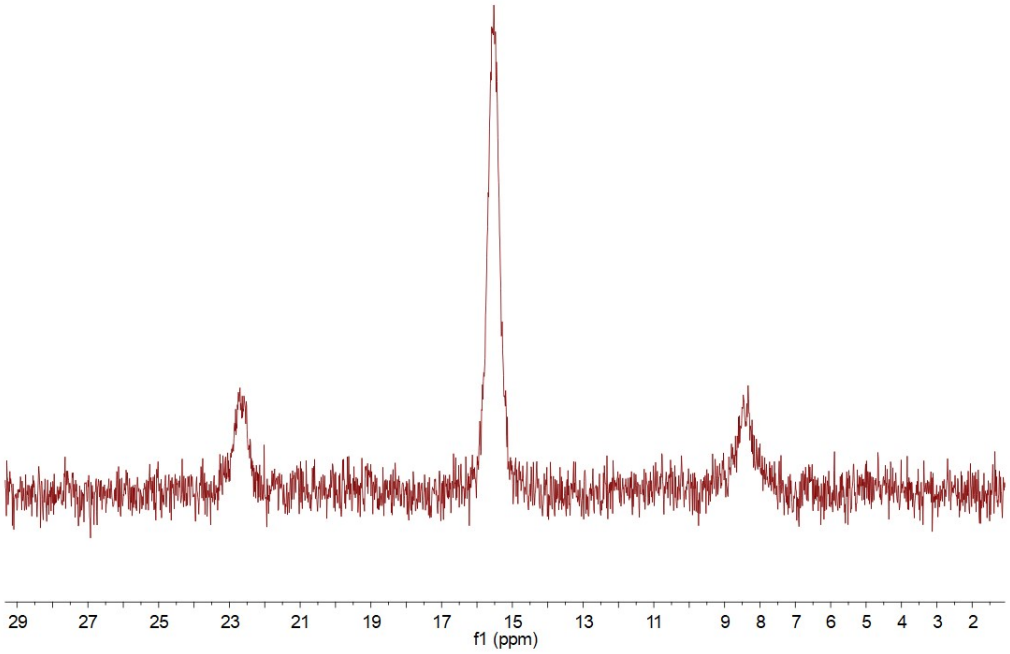

Figure S10. ^{31}P{^{1}H} NMR spectrum of **MPy1** in DMSO-d_6.

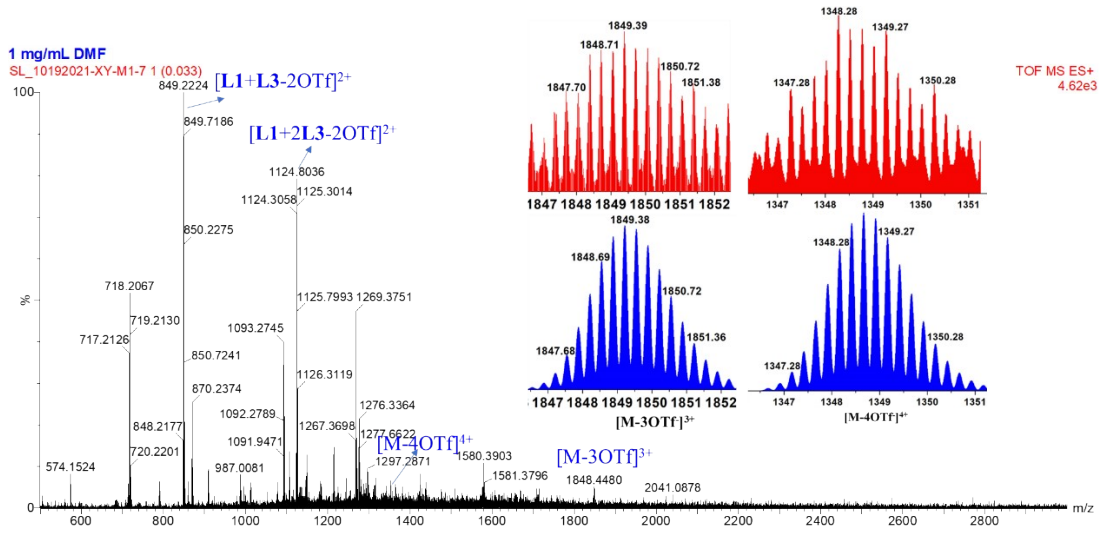

Figure S11. Experimental (red) and calculated (blue) electrospray ionization mass spectra of **MPy1**.

3. Synthesis of MPy2

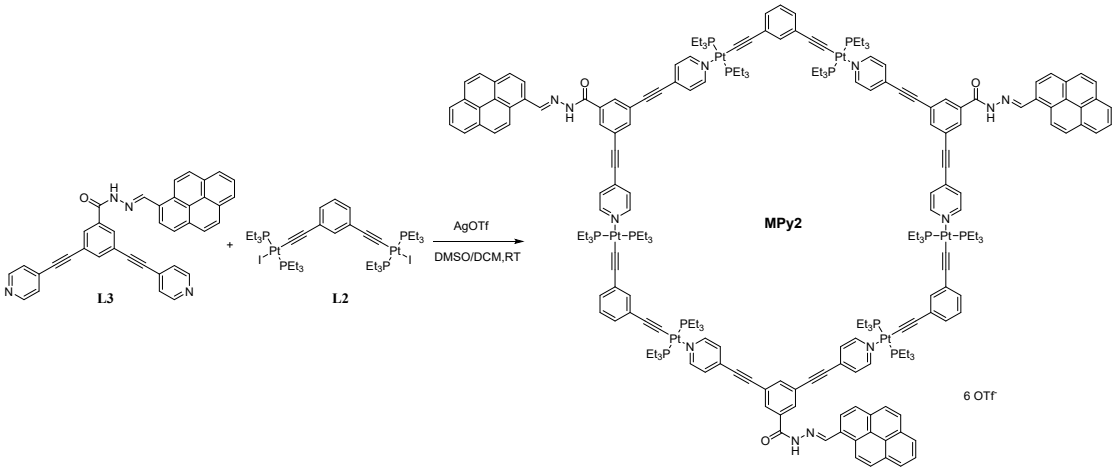

Figure S12. Synthesis route of **MPy2**.

L2 (10 mg, 7.0 μmol), AgOTf (5.5 mg, 21.0 μmol) and **L3** (4 mg, 7.0 μmol) were dissolved in the mixture of DMSO and DCM (2.0 mL, V_{DCM}:V_{DMSO} = 10:1) in a 20 mL glass vial. The reaction mixture was allowed to stir for 6 h at room temperature, and the reaction mixture was centrifuged at 3400 r/h for 20 min. To the resulting homogeneous solution, diethyl ether was added to precipitate the product, which was then isolated and dried under reduced pressure and re-dissolved in DMSO-d_6 for

characterization. ^{1}H NMR (400 MHz, DMSO-d_6) δ 12.31 (s, 1H), 9.55 (s, 1H), 8.96 – 8.81 (m, 5H), 8.62 (d, J = 8.1 Hz, 1H), 8.42 (d, J = 9.1 Hz, 4H), 8.37 – 8.14 (m, 6H), 7.89 (d, J = 15.6 Hz, 4H), 7.10 (s, 2H), 7.04 (s, 1H), 1.83 (s, 24H), 1.18 – 1.07 (m, 36H). ^{31}P NMR (121.4 MHz, DMSO-d_6) δ (ppm) 15.50 (s, ^{195}Pt satellites, $^{1}J_{Pt\text{-}P}$ = 1728.74 Hz). ESI-TOF-MS: $C_{222}H_{258}F_{18}N_{12}O_{21}P_{12}Pt_6S_6$ m/z [M-4OTf$^-$]$^{4+}$ 1231.28; [**L1**+2**L3**-2OTf]$^{2+}$ 1043.77; [**L1**+**L3**-2OTf]$^{2+}$ 768.18. (Where M represents the intact assembly).

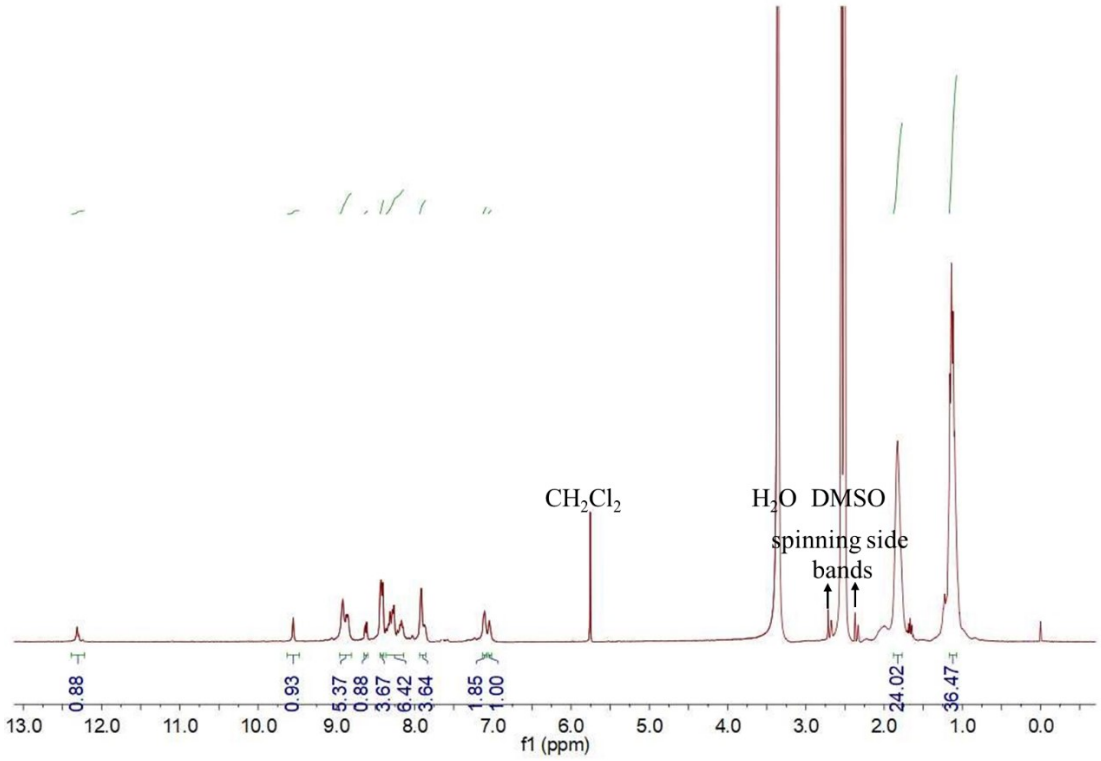

Figure S13. ^{1}H NMR spectrum of **MPy2** in DMSO-d_6.

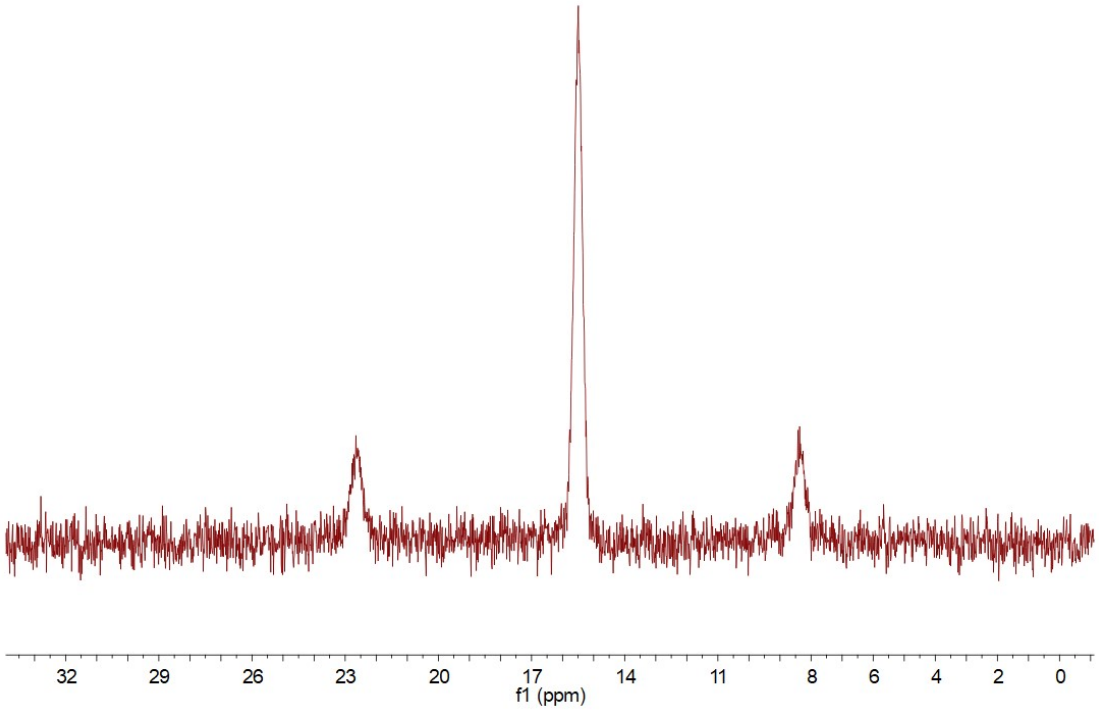

Figure. S14. $^{31}P\{^{1}H\}$ NMR spectrum of **MPy2** in DMSO-d_6.

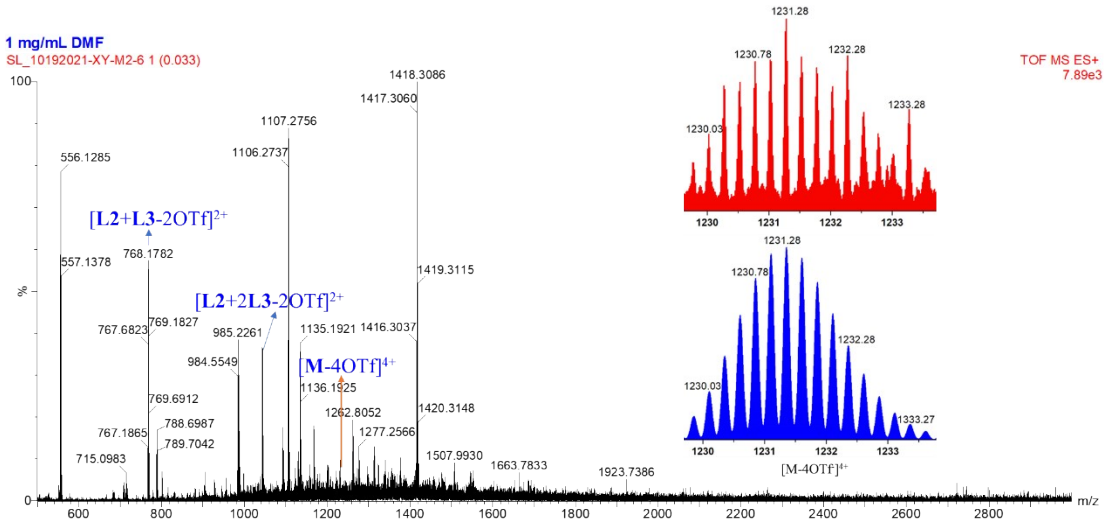

Figure S15. Experimental (red) and calculated (blue) electrospray ionization mass spectra of **MPy2.**

4. Synthesis of MPy3

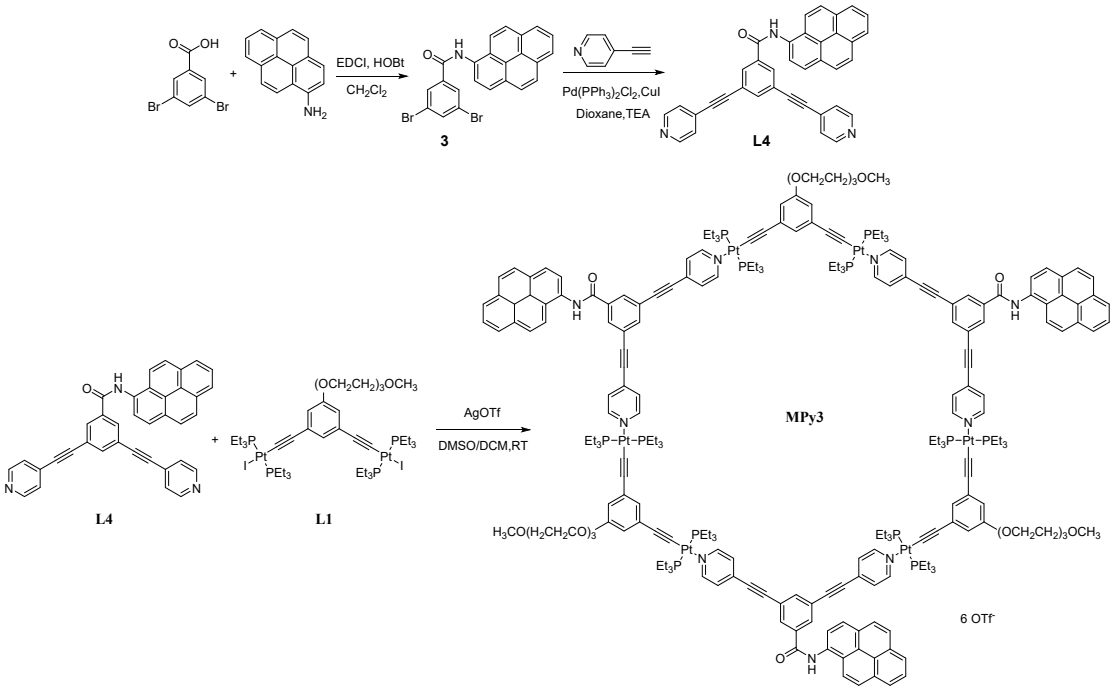

Figure S16. Synthesis route of **MPy3**.

Synthesis of 3

3,5-dibromobenzoic acid (140 mg, 1 eq), HOBt (148.6 mg, 1.1 eq), 1-ethyl- (3-dimethylaminopropyl) carbonyl diimidehydrochloride (EDCI) (210 mg, 1.1 eq) and triethylamine (300 mg, 3 eq) were added into a 50 mL two-necked flask and pumped under the protection of argon for three times. Then the newly steamed methylene chloride (20 mL) was added at 0 ℃. After stirring for 30 min in ice bath, 1-aminopyrene (93 mg, 0.8 mmol, 0.8 eq) dichloromethane solution was added drop by drop. After dropping, the solution was removed from the ice bath and reacted at room temperature for 24 h. The solvent was removed by reduced pressure, and the resulting mixture was dissolved with ethyl acetate and washed with water to remove water-soluble impurities. The residue was purified by column chromatography (silica, petroleum:ethyl acetate = 1:2 as the eluent) to obtain brown oily compound. ^{1}H NMR (400 MHz, DMSO-d_6) δ 10.99 (s, 1H), 8.36-8.10 (m, 12H). ^{13}C NMR (101 MHz, DMSO-d_6) δ 164.05, 138.55, 136.87, 131.66, 131.22, 130.94, 130.43, 129.68, 127.83,

127.70, 127.60, 126.97, 126.09, 125.92, 125.71, 125.51, 125.40, 124.83, 124.23, 123.40, 123.20. ESI-MS: m/z Calcd for $C_{23}H_{13}Br_2NO$ $[M+H]^+$ 477.9, found 477.9.

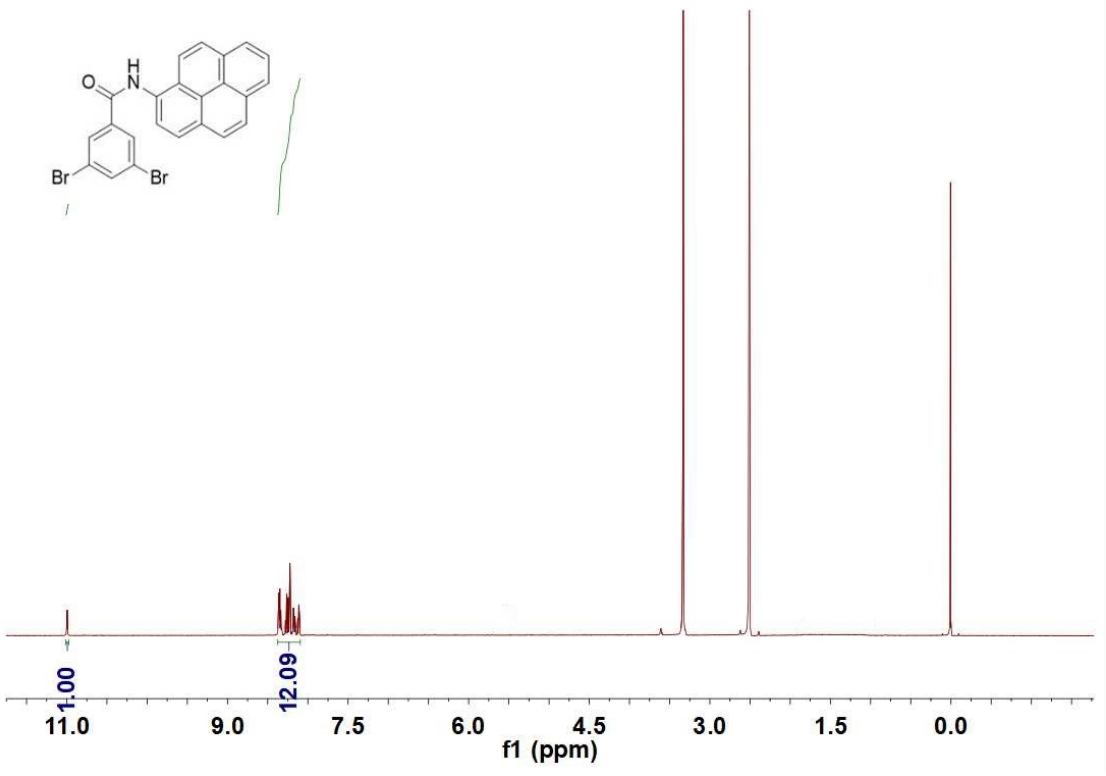

Figure S17. ^{1}H NMR spectrum of **3** in DMSO-d_6.

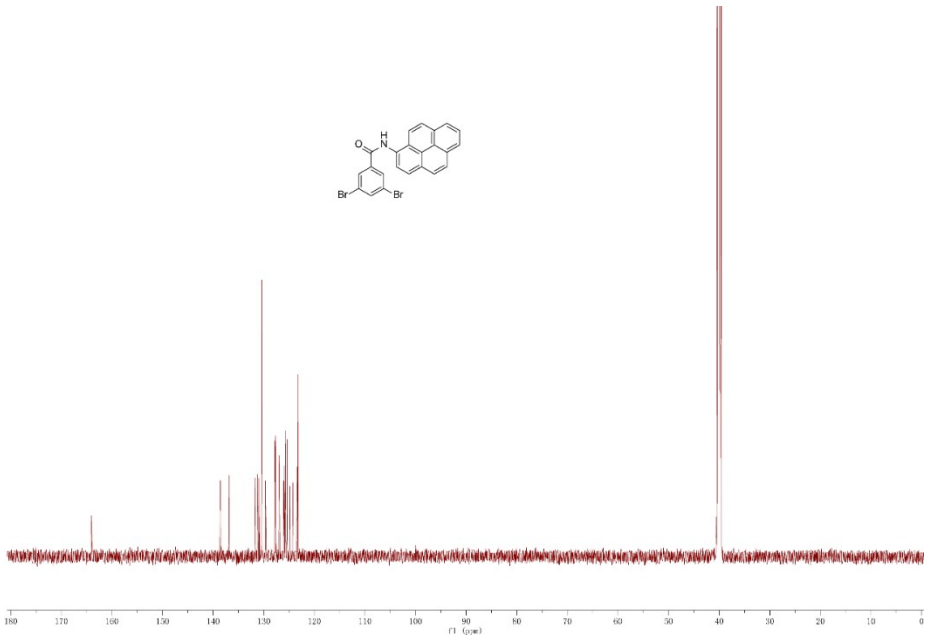

Figure S18. ^{13}C NMR spectrum of **3** in DMSO-d_6.

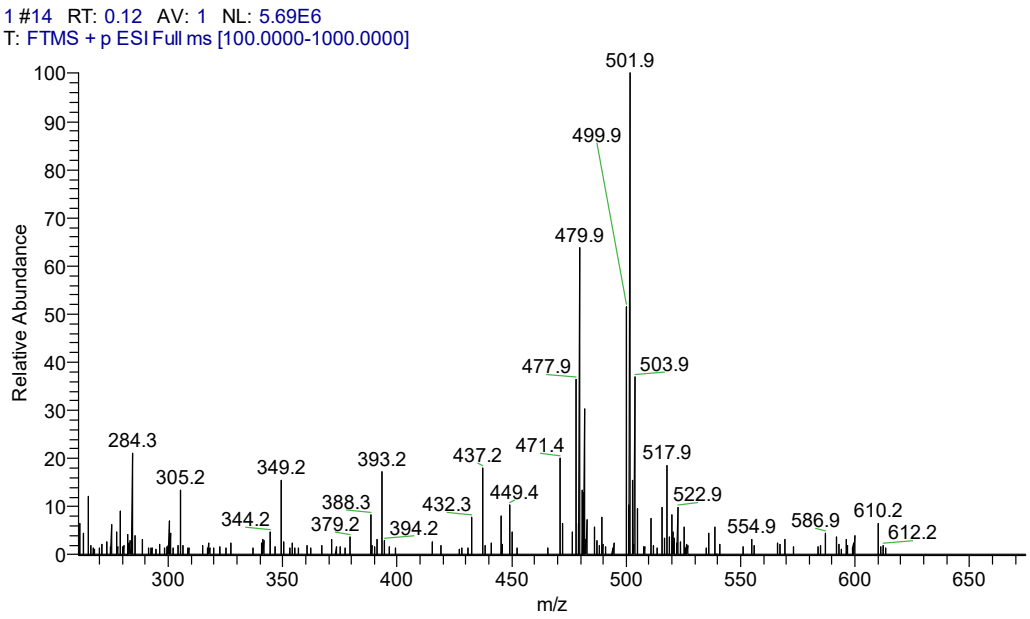

Figure S19. ESI spectrum of compound **3**.

Synthesis of L4

A Schlenk tube was charged with **3** (250 mg, 0.85 mmol), 4-ethynylpyridine hydrochloride (263 mg, 2.55 mmol), $Pd(PPh_3)Cl_2$ (140 mg, 0.2 mmol), and CuI (32.4 mg, 0.17 mmol). The mixture was placed under nitrogen atmosphere, and anhydrous triethylamine (15 mL) and 1,4-dioxane (10 mL) were added by syringe. The reaction was heated at 85 ℃ for 48 h under nitrogen, then cooled down to room temperature and the solvents were removed under reduced pressure. The residue was dissolved in dichloromethane (200 mL) and washed by water (150 mL). After drying over Na_2SO_4, the solvent was removed and the residue was purified by column chromatography on silica gel (EA/petroleum ether = 1:1) to afford **L4** as a yellow powder. Yield: 187 mg, 59%. ^{1}H NMR (400 MHz, DMSO-d_6) δ 11.12 (s, 1H), 8.76 (s, 4H), 8.55-8.29 (m, 9H), 8.27-8.21 (m, 2H), 8.18 (d, J = 7.6 Hz, 1H), 7.68 (d, J = 5.0 Hz, 4H). ^{13}C NMR (400 MHz, DMSO-d_6) δ 164.05, 150.09, 138.55, 131.66, 131.22, 130.42, 129.68, 127.83, 127.70, 127.60, 126.97, 126.09, 125.91, 125.71, 125.51, 125.40, 124.83, 124.23, 123.40, 123.20, 86.30, 80.10. ESI-MS: m/z Calcd for $C_{37}H_{21}N_3O$ $[M+H]^+$ 524.2, found 524.2.

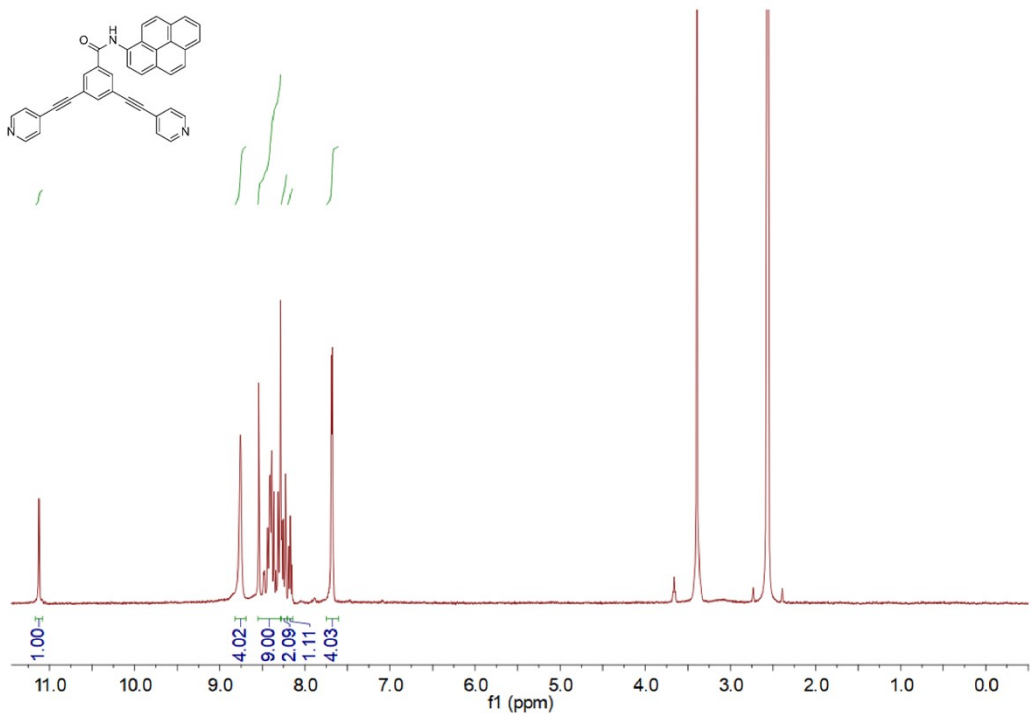

Figure S20. ^{1}H NMR spectrum of **L4** in DMSO-d_6.

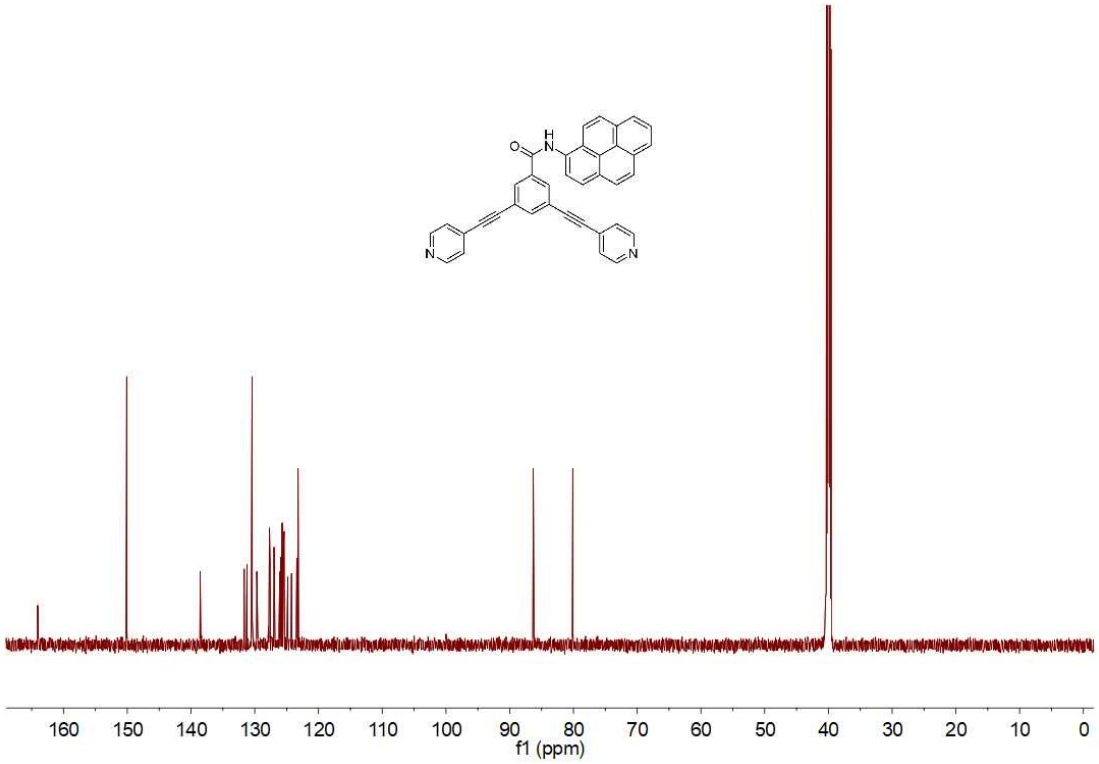

Figure S21. ^{13}C NMR spectrum of **L4** in DMSO-d_6.

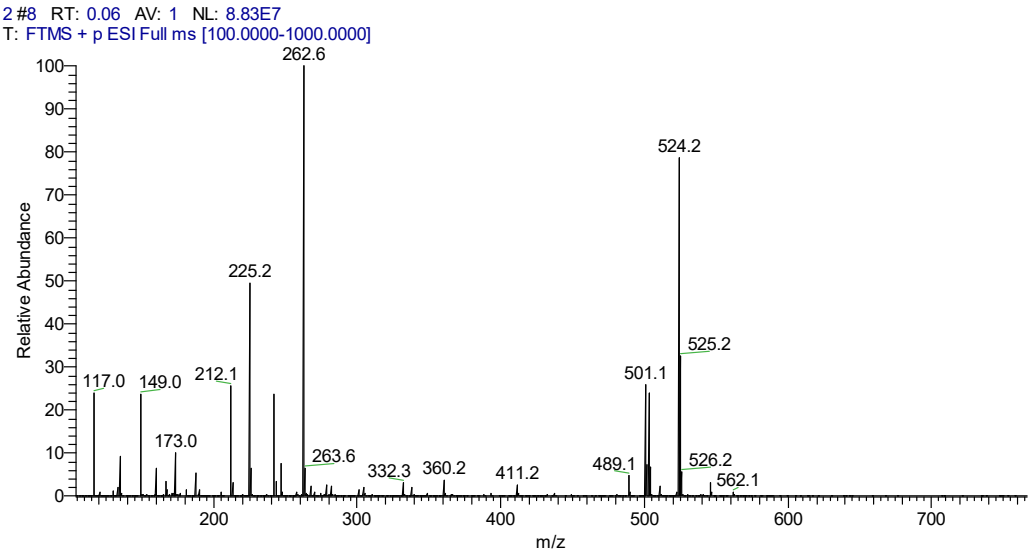

Figure S22. ESI spectrum of compound **L4**.

Synthesis of MPy3

L1 (10 mg, 7.0 μmol), AgOTf (5.5 mg, 21.0 μmol) and **L4** (4 mg, 7.0 μmol) were dissolved in the mixture of DMSO and DCM（2.0 mL, V_{DCM}:V_{DMSO}=10:1) in a 20 mL glass vial. The reaction mixture was allowed to stir for 6 h at room temperature, and the reaction mixture was centrifuged at 3400 r/h for 20 min. To the resulting homogeneous solution, diethyl ether was added to precipitate the product, which was then isolated and dried under reduced pressure and re-dissolved in DMSO-d_6 for characterization. ^{1}H NMR (400 MHz, DMSO-d_6) δ 11.08 (s, 1H), 8.90 (s, 4H), 8.60 (s, 1H), 8.4 – 8.2 (m, 11H), 7.90 (s, 4H), 6.63 (s, 2H), 6.56 (s, 1H), 4.05 (s, 2H), 3.72 (s, 2H), 3.61 – 3.49 (m, 6H), 3.43 (s, 2H), 3.24 (s, 3H), 1.81 (s, 24H), 1.15 – 1.05 (m, 36H). ^{31}P NMR (121.4 MHz, DMSO-d_6) δ (ppm) 15.52 (s, ^{195}Pt satellites, $^1J_{Pt\text{-}P}$ = 1731.16 Hz). $C_{240}H_{297}F_{18}N_9O_{33}P_{12}Pt_6S_6$ m/z [M-3OTf]$^{3+}$ 1821.38; [M-4OTf]$^{4+}$ 1328.80; [**L1**+2**L4**-2OTf]$^{2+}$ 1097.77; [M-5OTf]$^{5+}$ 1033.23; [**L1**+**L4**-2OTf]$^{2+}$ 835.70. (Where M represents the intact assembly).

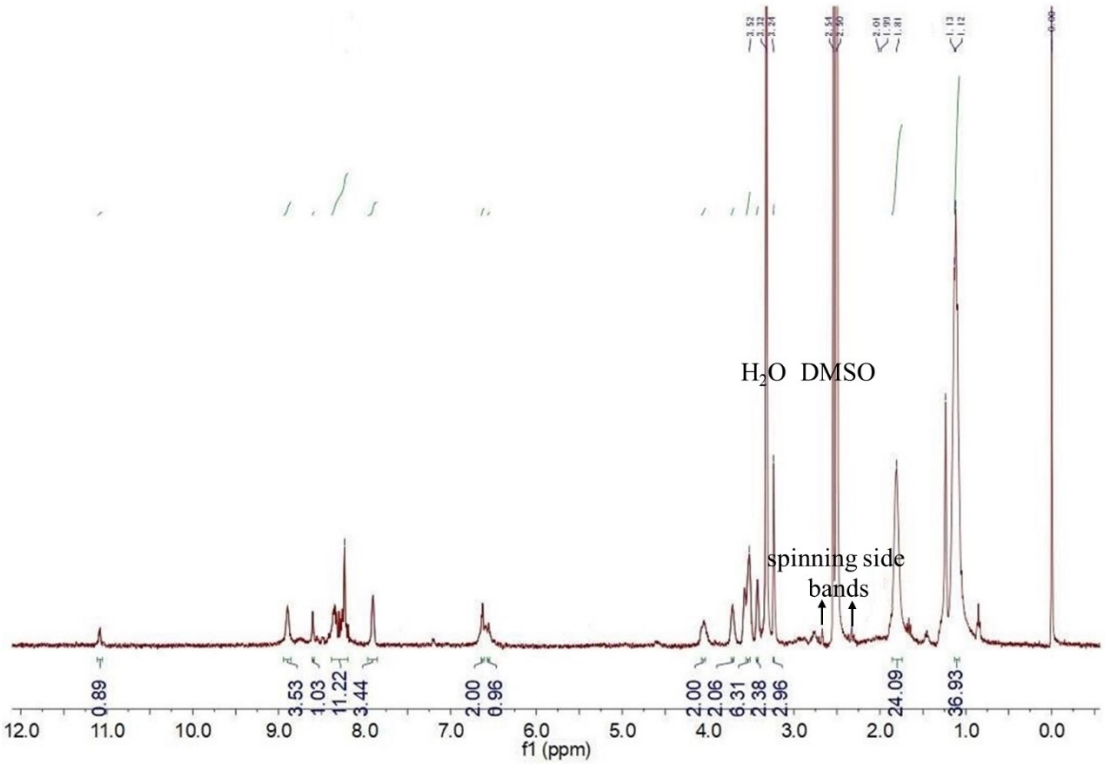

Figure S23. ^{1}H NMR spectrum of **MPy3** in DMSO-d_6.

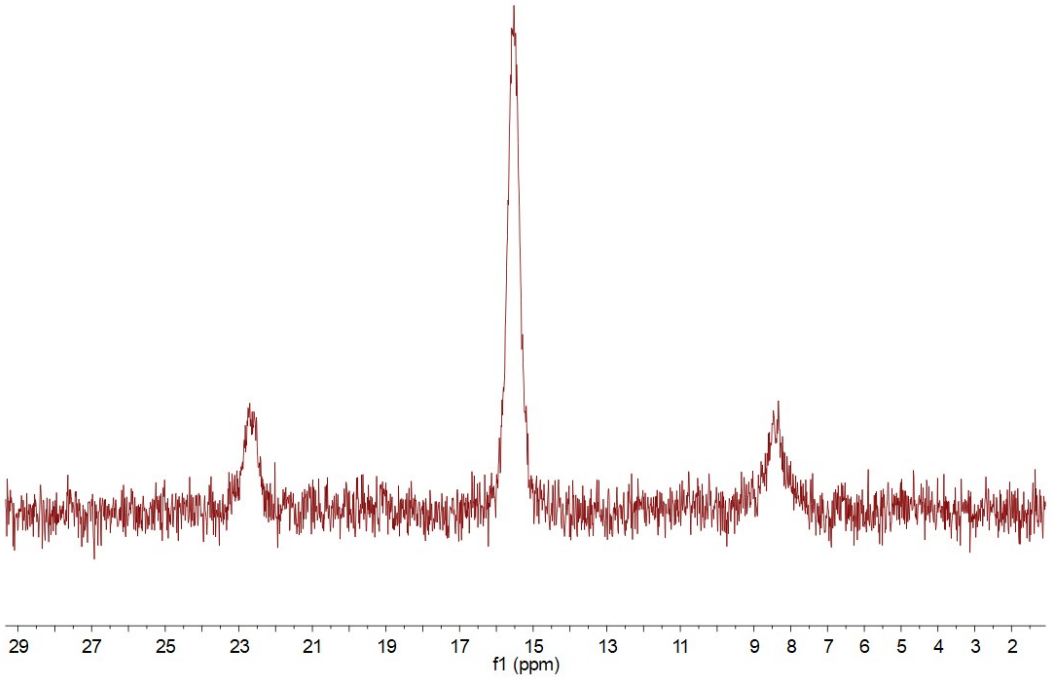

Figure S24. ^{31}P{^{1}H} NMR spectrum of **MPy3** in DMSO-d_6.

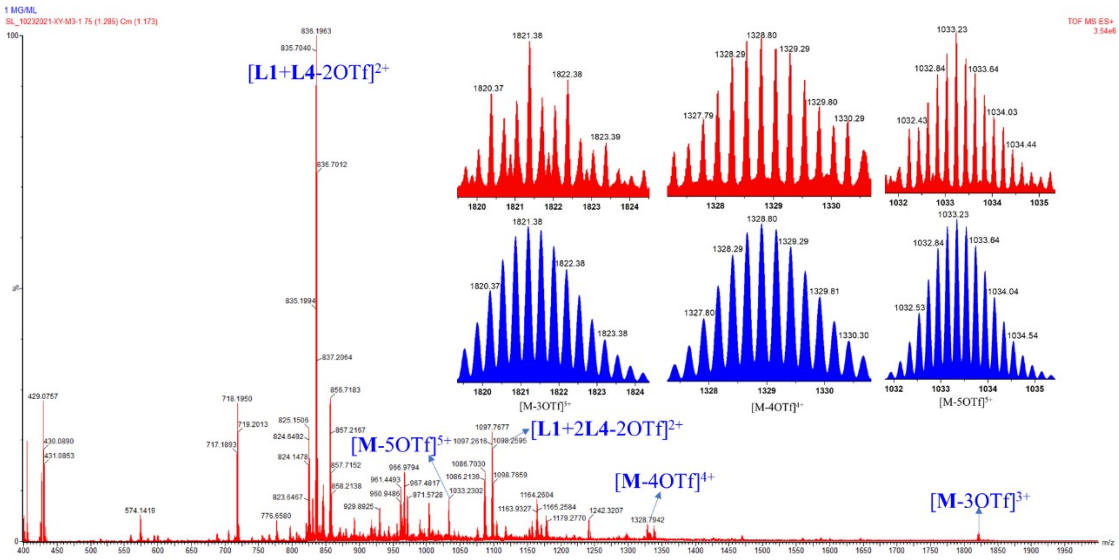

Figure S25. Experimental (red) and calculated (blue) electrospray ionization mass spectra of **MPy3.**

5. Synthesis of MPy4

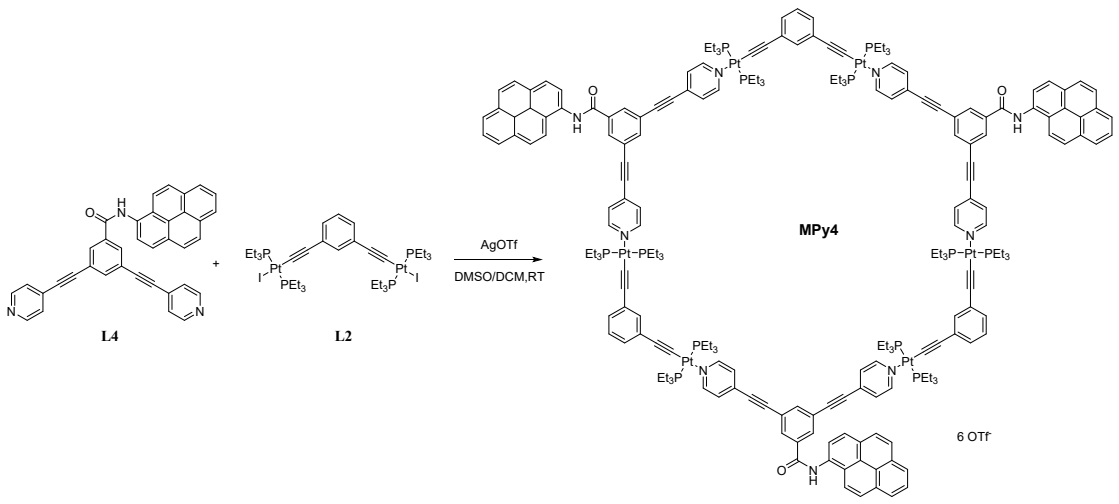

Figure S26. Synthesis route of **MPy4**.

Synthesis of MPy4

L2 (10 mg, 7.0 μmol), AgOTf (5.5 mg, 21.0 μmol) and **L4** (4 mg, 7.0 μmol)

were dissolved in the mixture of DMSO and CH_2Cl_2 (2.0 mL, V_{CH2Cl2}:V_{DMSO} = 10:1) in a 20 mL glass vial. The reaction mixture was allowed to stir for 6 h at room temperature, and the reaction mixture was centrifuged at 3400 r/h for 20 min. To the resulting homogeneous solution, diethyl ether was added to precipitate the product, which was then isolated and dried under reduced pressure and re-dissolved in DMSO-d_6 for characterization. ^{1}H NMR (400 MHz, DMSO-d_6) δ 11.09 (s, 1H), 8.90 (s, 4H), 8.60 (s, 2H), 8.38 – 8.12 (m, 10H), 7.90 (s, 4H), 7.10 (d, J = 7.8 Hz, 2H), 7.03 (s, 1H), 1.82 (s, 24H), 1.12 – 1.06 (m, 36H). ^{31}P NMR (121.4 MHz, DMSO-d_6) δ (ppm) 15.48 (s, ^{195}Pt satellites, $^1J_{Pt\text{-}P}$ = 1734.81 Hz). ESI-TOF-MS: $C_{219}H_{255}F_{18}N_9O_{21}P_{12}Pt_6S_6$ m/z [M-3OTf]$^{3+}$ 1659.25; [M-4OTf]$^{4+}$ 1207.19; [**L2**+2**L4**-2OTf]$^{2+}$ 1016.68; [M-5OTf]$^{5+}$ 936.16; [**L2**+**L4**-2OTf]$^{2+}$ 755.13. (Where M represents the intact assembly).

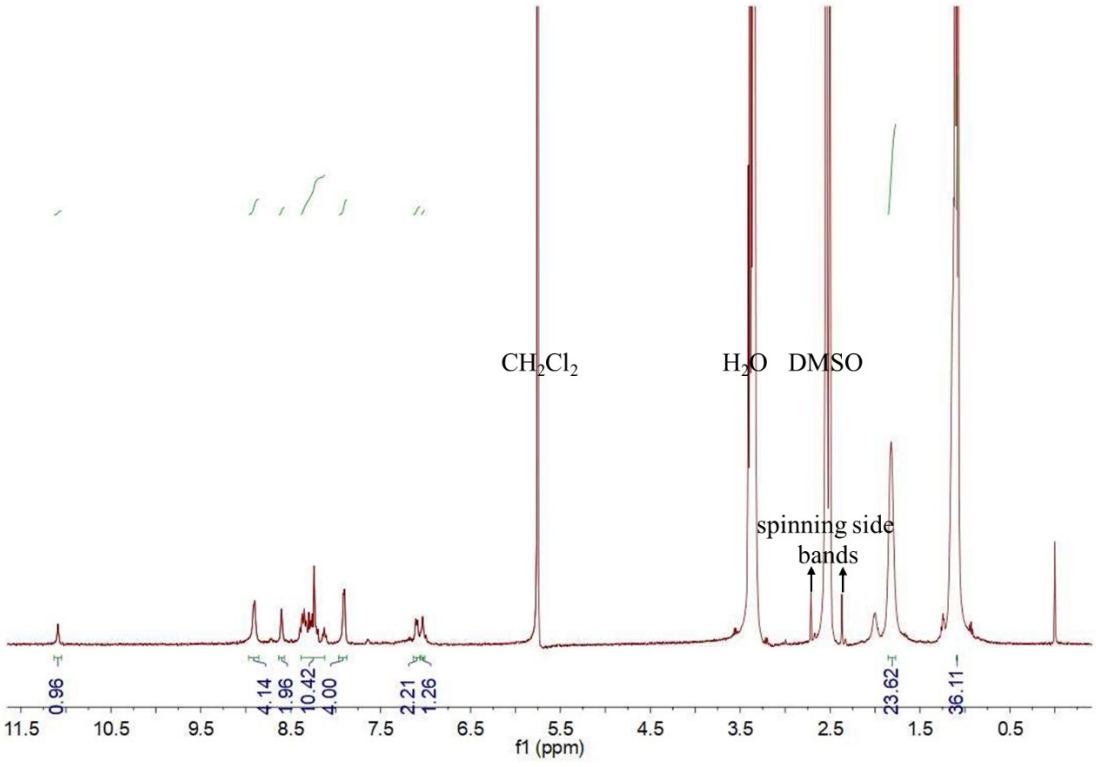

Figure S27. ^{1}H NMR spectrum of **MPy4** in DMSO-d_6.

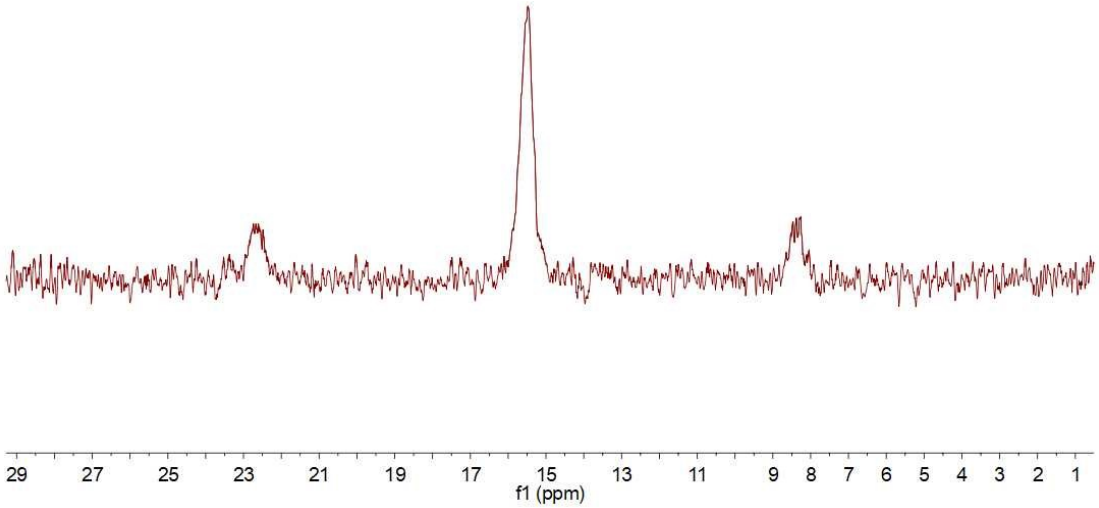

Figure S28. $^{31}P\{^{1}H\}$ NMR spectrum of **MPy4** in DMSO-d_6.

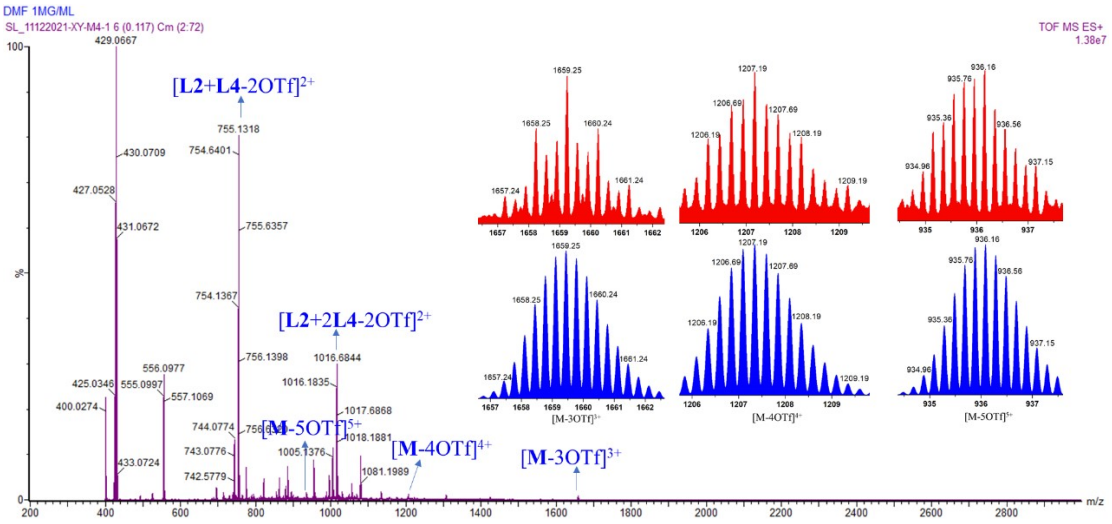

Figure S29. Experimental (red) and calculated (blue) electrospray ionization mass spectra of **MPy4.**

6. Experimental procedure and methods

6.1 The preparation of the samples

The preparation process for the assembly: the stock solution of **MPy1** (2×10^{-4} M, dissolved in DMSO), ESY (1×10^{-5} M, dissolved in H_2O−DMSO, v/v; 3:2), SR101

(1×10^{-5} M, dissolved in H_2O−DMSO, v/v; 3:2) were prepared, respectively. **MPy1** assembly was prepared as follows: 0.2 mL of **MPy1** stock solution was added into the mixture of water (2.4 mL) and DMSO (1.4 mL) under stirring to afford 1×10^{-5} M solution (H_2O−DMSO, v/v; 3:2). **MPy1**-ESY assembly was prepared as follows: 20 μL of ESY stock solution was added into 2 mL of **MPy1** assembly. **MPy1**-SR101 assembly was prepared as follows: 20 μL of SR101 stock solution was added into 2 mL of **MPy1** assembly. **MPy1**-ESY-SR101 assembly was prepared as follows: 10 μL of SR101 solution was added into 2 mL of **MPy1**-ESY assembly (100:1).

The fluorescence experiments were conducted as follows: ESY and SR101 was dissolved in H_2O−DMSO (3:2; v/v) and added into the H_2O−DMSO mixture of **MPy1** or **MPy1-ESY** assembly (100:1), respectively.

6.2 The measurement of the Tyndall effect

As shown in **6.1**, the solution of **MPy1**, **MPy1**-ESY (100:1) and **MPy1**-ESY-SR101 (200:2:1) in H_2O−DMSO (3:2; v/v) was prepared, [**MPy1**] = 1.0×10^{-6} M, [ESY] = 1.0×10^{-8} M, [SR101] = 5.0×10^{-9} M, using a laser pointer to send a beam of light through cuvette, which were photographed under 365 nm UV light.

6.3 Preparation of anti-counterfeiting inks

The luminescent printing was performed with a modified HP Deskjet 1112 inkjet printer. The conventional inkjet office printer cartridge (HP 803) was refitted first. After removal of ink, the cartridge was thoroughly cleared with water and ethanol until it was clean, and dried by blowing with N_2 at room temperature. The fluorescent ink (**MPy1**−ESY−SR101 system at different donor/acceptor ratios) was injected into the cartridge, and then different patterns were printed as designed on unmodified copy paper.

6.4 Energy transfer efficiency (Φ_{ET})

The energy-transfer efficiency (Φ_{ET}) was calculated using equation S1.

$$\Phi_{ET}=1-I_{DA,\,(\lambda ex=donor)}/I_{D,\,(\lambda ex=donor)} \qquad \textbf{(eq. S1)}$$

For **MPy1**–ESY system, where $\mathbf{I_{DA}}$ and $\mathbf{I_D}$ are the fluorescence intensity of **MPy1**–ESY assembly (donor and acceptor) and **MPy1** assembly (donor) at 460 nm when excited at 384 nm, respectively. The energy-transfer efficiency (Φ_{ET}) was calculated as 12.2 % in H_2O–DMSO (3:2; v/v), measured under the condition of [**MPy1**] = 1.0×10^{-5} M, [ESY] = 1.0×10^{-7} M, and λ_{ex} = 384 nm.

For **MPy1**–SR101 system, where $\mathbf{I_{DA}}$ and $\mathbf{I_D}$ are the fluorescence intensity of **MPy1**–**SR101** assembly (donor and acceptor) and **MPy1** assembly (donor) at 460 nm when excited at 384 nm, respectively. The energy-transfer efficiency (Φ_{ET}) was calculated as 2.3 % in H_2O–DMSO (3:2; v/v), measured under the condition of [**MPy1**] = 1.0×10^{-5} M, [SR101] = 1.0×10^{-7} M, and λ_{ex} = 384 nm.

For **MPy1**–**ESY**–**SR101** system, where $\mathbf{I_{DA}}$ and $\mathbf{I_D}$ are the fluorescence intensity of **MPy1**–**ESY**–**SR101** assembly (donor and acceptor) and **MPy1**–**ESY** assembly (donor) at 550 nm when excited at 384 nm, respectively. The energy-transfer efficiency (Φ_{ET}) was calculated as 20.1 % in H_2O–DMSO (3:2; v/v), measured under the condition of [**MPy1**] = 1.0×10^{-5} M, [**ESY**] = 1.0×10^{-7} M, [**SR101**] = 5.0×10^{-8} M, and λ_{ex} = 384 nm.

6.5 Antenna effect (AE)

The antenna effect (AE) was calculated using equation S2.

$$\textbf{Antenna effect} = (\mathbf{I_{DA,\,(\lambda ex=donor)}} - \mathbf{I_{D,\,(\lambda ex=donor)}})/\mathbf{I_{DA,\,(\lambda ex=acceptor)}} \qquad \textbf{(eq. S2)}$$

Where $I_{DA,\,(\lambda ex=donor)}$ and $I_{DA,\,(\lambda ex\,=acceptor)}$ are the fluorescence intensity of the system with excitation of donor and direct excitation of acceptor, respectively. $I_{D,\,(\lambda ex=donor)}$ is the fluorescence intensity of the donor.

For **MPy1**–**ESY** system, where $I_{DA,\,(\lambda ex=donor)}$ and $I_{DA,\,(\lambda ex=acceptor)}$ are the fluorescence intensity at 550 nm with the excitation of the donor at 384 nm and the direct excitation of the acceptor at 500 nm, respectively. $I_{D,\,(\lambda ex=\ donor)}$ is the fluorescence intensity at 550 nm of the **MPy1** assembly, which was normalized with the **MPy1**–**ESY** assembly at 460 nm. The antenna effect value was calculated as 14.3 in H_2O–DMSO (3:2; v/v), measured under the condition of [**MPy1**] = 1.0×10^{-5} M, [ESY] = 1.0×10^{-7} M, and λ_{ex} = 384 nm (Figure S56).

For **MPy1**–SR101 system, where $I_{DA,\ (\lambda ex=donor)}$ and $I_{DA,\ (\lambda ex=acceptor)}$ are the fluorescence intensity at 610 nm with the excitation of the donor at 384 nm and the direct excitation of the acceptor at 580 nm, respectively. $I_{D,\ (\lambda ex=donor)}$ is the fluorescence intensity at 610 nm of the **MPy1** assembly, which was normalized with the **MPy1**−SR101 assembly at 460 nm. The antenna effect value was calculated as 5.8 in H_2O−DMSO (3:2; v/v), measured under the condition of [**MPy1**] = 1.0×10^{-5} M, [SR101] = 1.0×10^{-7} M, and λ_{ex} = 384 nm (Figure S56).

For **MPy1**–ESY–SR101 system, where $I_{DA,\ (\lambda ex=donor)}$ and $I_{DA,\ (\lambda ex=acceptor)}$ are the fluorescence intensities at 610 nm with the excitation of the donor at 384 nm and the direct excitation of the acceptor at 580 nm, respectively. $I_{D,\ (\lambda ex=\ donor)}$ is the fluorescence intensities at 610 nm of the **MPy1**−ESY assembly, which was normalized with the **MPy1**−ESY−SR101 assembly at 550 nm. The antenna effect value was calculated as 9.3 in H_2O−DMSO (3:2; v/v), measured under the condition of [**MPy1**] = 1.0×10^{-5} M, [ESY] = 1.0×10^{-7} M, [SR101] = 5.0×10^{-8} M, and λ_{ex} = 384 nm (Figure S58).

7. Additional tables

Table S1. Fluorescence lifetimes of **MPy1**, **MPy1**−ESY and **MPy1**−ESY−SR101 assemblies in H_2O−DMSO (3:2; v/v).

Sample	τ_1/ns	Rel %	τ_2/ns	Rel %	A	χ^2
MPy1 (solid)	1.64	41.45	5.39	58.55	4.118	1.237
MPy1[a]	1.64	39.07	5.35	60.93	4.308	1.208
MPy1−ESY (300:1)[a]	1.47	31.23	4.90	68.77	3.210	1.212
MPy1−ESY (100:1)[a]	1.30	29.50	4.56	70.50	1.794	1.158
MPy1−ESY (100:1)[b]	1.28	71.32	4.78	28.68	1.482	1.283
MPy1−ESY−SR101 (200:2:0.5)[b]	1.19	58.21	4.34	41.79	2.115	1.278
MPy1−ESY−SR101	1.19	65.28	3.73	34.72	4.087	1.287

(200:2:1)[b]						

a: monitored at 460 nm upon excitation at 375 nm; [**MPy1**] = 1.0×10^{-5} M, [ESY] = 1.0×10^{-7} M.

b: monitored at 550 nm upon excitation at 375 nm; [**MPy1**] = 1.0×10^{-5} M, [ESY] = 1.0×10^{-7} M, [SR101] = 5.0×10^{-8} M, (Figures S31, S47-S52).

Table S2. Fluorescence quantum yields of ESY in H_2O−DMSO (3:2; v/v), SR101 in H_2O−DMSO (3:2; v/v), **MPy1** (in DMSO solution), **MPy1** (solid), **MPy1**−ESY and **MPy1**−ESY−SR101 in H_2O−DMSO (3:2; v/v).

Sample	Concentration	Fluorescence quantum yields (Φ_f)
ESY	[ESY] = 1.0×10^{-5} M	38.86%
SR101	[SR101] = 1.0×10^{-5} M	81.58%
MPy1 in DMSO solution	[**MPy1**] = 1.0×10^{-5} M	0.98%
MPy1 in the solid state	-	0.02%
MPy1	[**MPy1**] = 1.0×10^{-5} M	13.2 %
MPy1−ESY	[**MPy1**] = 1.0×10^{-5} M [ESY] = 1.0×10^{-7} M	17.4 %
MPy1−SR101	[**MPy1**] = 1.0×10^{-5} M [SR101] = 1.0×10^{-7} M	9.11 %
MPy1−ESY−SR101	[**MPy1**] = 1.0×10^{-5} M [ESY] = 1.0×10^{-7} M [SR101] = 5.0×10^{-8} M	21.3 %

Table S3. The energy transfer efficiency in H_2O−DMSO (3:2; v/v).

Sample	Concentration	energy transfer efficiency

		(Φ_{ET})
MPy1−ESY (100:1)	[**MPy1**] = 1.0×10^{-5} M [ESY] = 1.0×10^{-7} M	12.2 %
MPy1−SR101 (100:1)	[**MPy1**] = 1.0×10^{-5} M [SR101] = 1.0×10^{-7} M	2.3 %
MPy1−ESY−SR101 (200:2:1)	[**MPy1**] = 1.0×10^{-5} M [ESY] = 1.0×10^{-7} M [SR101] = 5.0×10^{-8} M	20.1 %

Table S4. Antenna effect

Sample	Concentration	Antenna effect
MPy1−ESY (100:1)	[**MPy1**] = 1.0×10^{-5} M [ESY] = 1.0×10^{-7} M	14.3
MPy1−SR101 (100:1)	[MPy1] = 1.0×10^{-5} M [SR101] = 1.0×10^{-7} M	5.8
MPy1−ESY−SR101 (200:2:1)	[**MPy1**] = 1.0×10^{-5} M [ESY] = 1.0×10^{-7} M [SR101] = 5.0×10^{-8} M	9.3

8. Additional Spectra and images

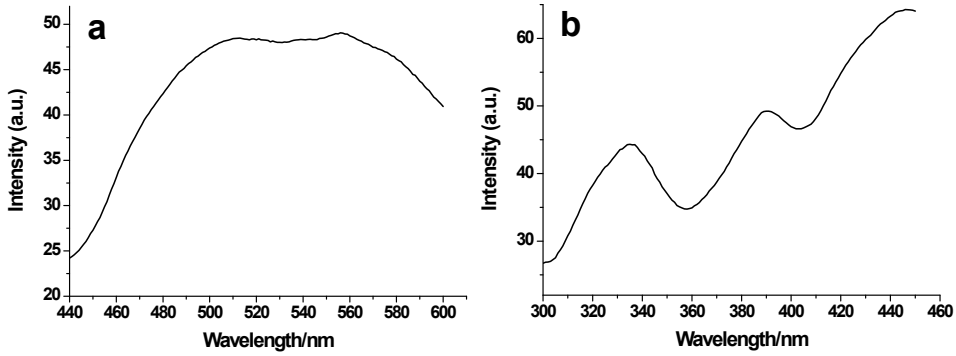

Figure S30. The emission of **MPy1** on λ_{ex} 390 nm (a) and excitation spectrum for λ_{em} 530 nm (b) in the solid state.

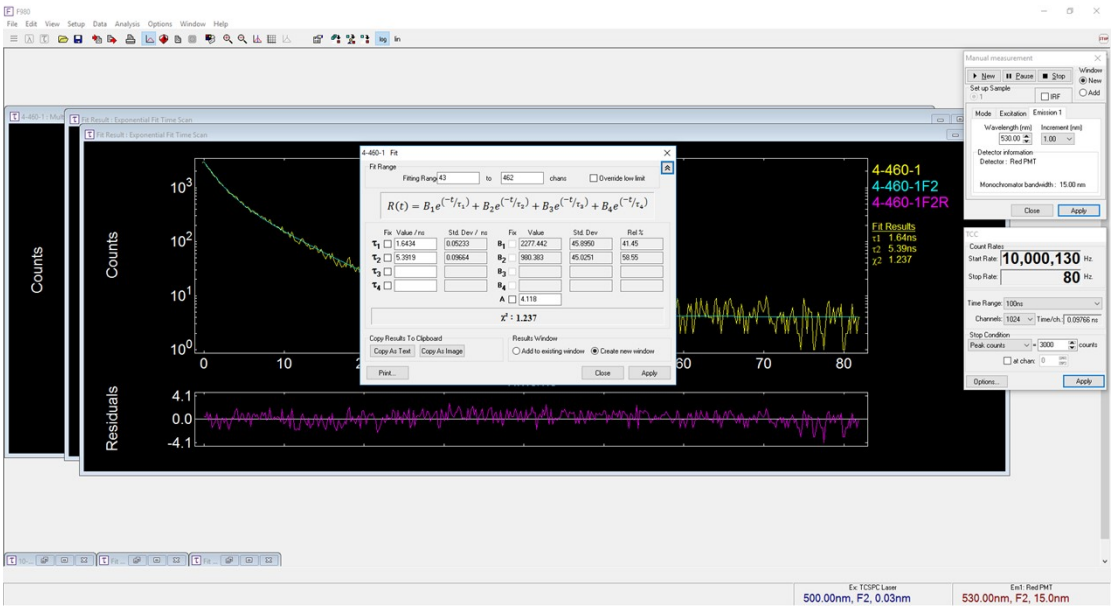

Figure S31. Fluorescence decay profiles of **MPy1** (λ_{ex} = 390 nm, $\lambda_{collected}$ = 530 nm) in the solid state.

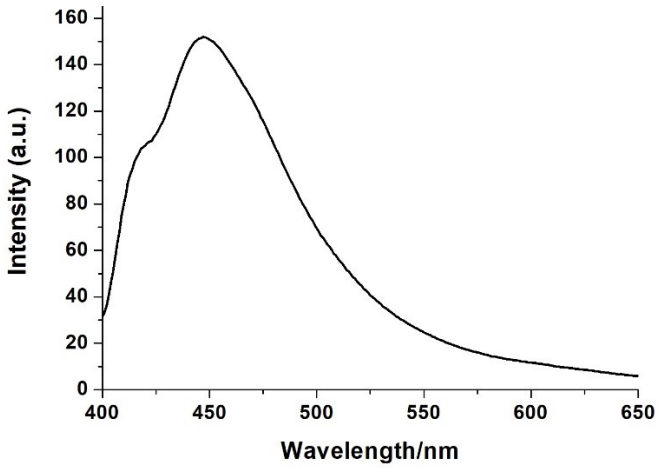

Figure S32. Fluorescence spectrum of **MPy1** in THF (1% DMSO) at 298 K (λ_{ex} = 390 nm).

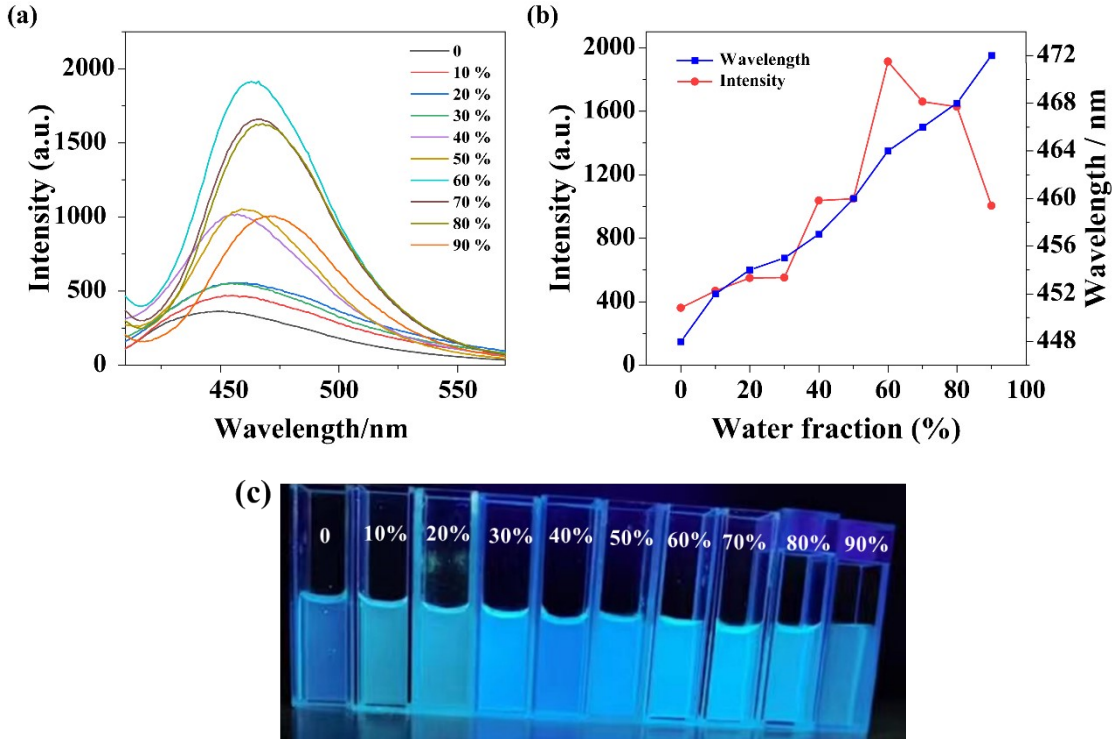

Figure S33. (a) Fluorescence spectra of **MPy1** in H_2O−DMSO mixtures with different water volume fractions (*f*w, vol %) (λ_{ex} = 384 nm). (b) Fluorescence intensity and emission wavelength of **MPy1** with various fractions of water from 0 to 90 %. (c) Photographs of **MPy1** with various fractions of water under 365 nm irradiation.

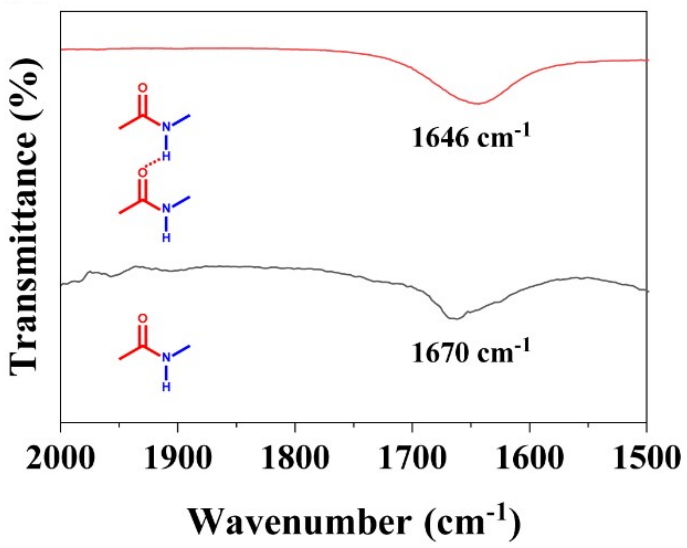

Figure S34. FTIR spectra of compound **MPy1** (10 mM) in DMSO (black line) and H_2O−DMSO (3:2; v/v) (red line). The sharp amide I band shifted from 1670 cm^{-1} in

DMSO (monomers) to 1646 cm^{-1} in H_2O−DMSO (3:2; v/v) (aggregation), suggesting the formation of intermolecular hydrogen bonds.

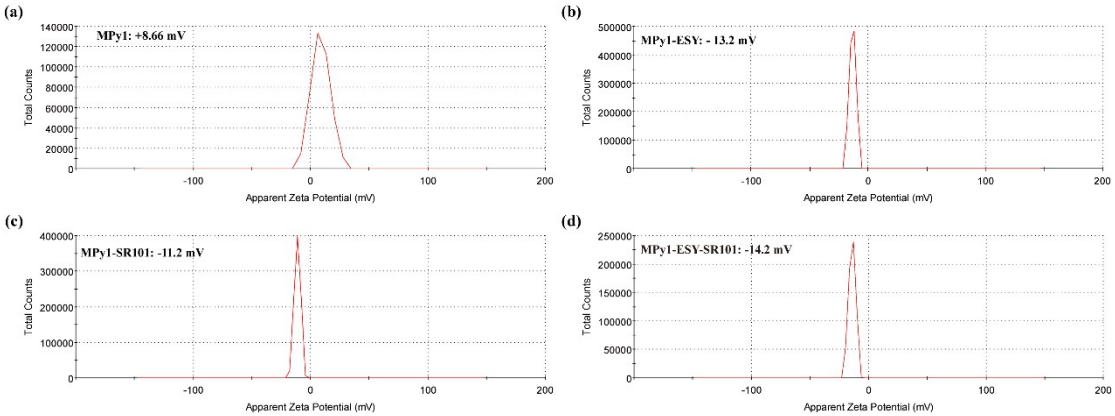

Figure S35. Zeta potentials of **MPy1**, **MPy1**−ESY (100:1), **MPy1**−SR101 (100:1) and **MPy1**−ESY−SR101 (200:2:1) in H_2O−DMSO (3:2; v/v).

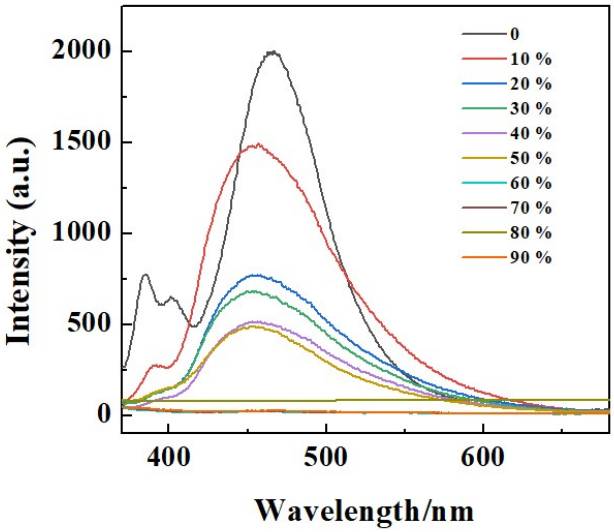

Figure S36. Fluorescence spectra of **L3** in H_2O−DMSO mixtures with different water volume fractions (*f*w, vol %) (λ_{ex} = 350 nm).

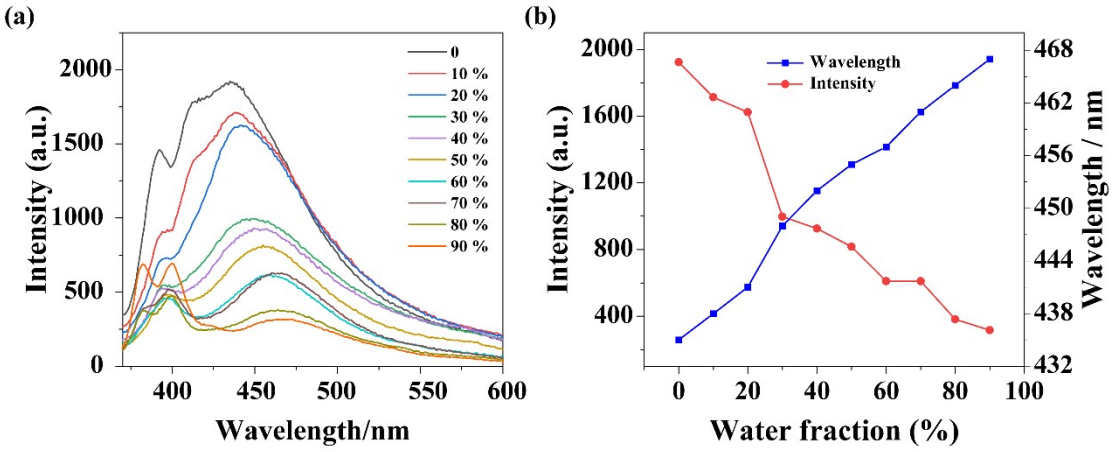

Figure S37. (a) Fluorescence spectra of **MPy2** in H_2O−DMSO mixtures with different water volume fractions (f_W, vol %) (λ_{ex} = 350 nm). (b) Fluorescence intensity of **MPy2** with various fractions of water from 0 to 90 %.

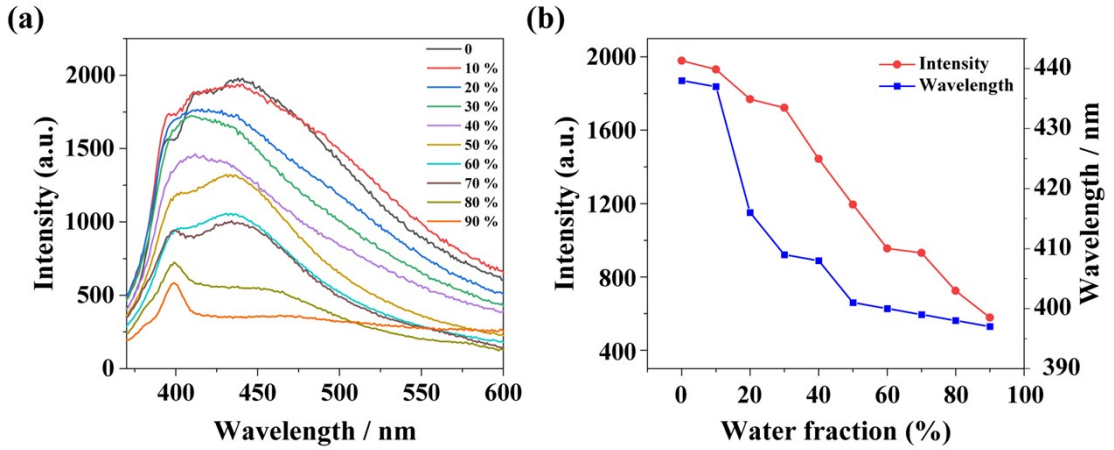

Figure S38. (a) Fluorescence spectra of **MPy4** in H_2O−DMSO mixtures with different water volume fractions (f_W, vol %) (λ_{ex} = 350 nm). (b) Fluorescence intensity of **MPy4** with various fractions of water from 0 to 90 %.

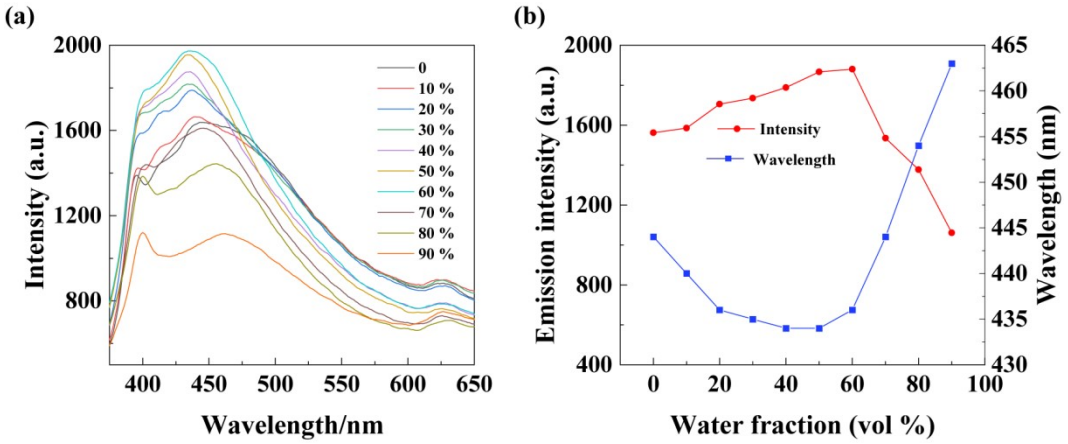

Figure S39. (a) Fluorescence spectra of **MPy3** in H_2O−DMSO mixtures with different water volume fractions (f_W, vol %) (λ_{ex} = 350 nm). (b) Fluorescence intensity of **MPy3** with various fractions of water from 0 to 90 %.

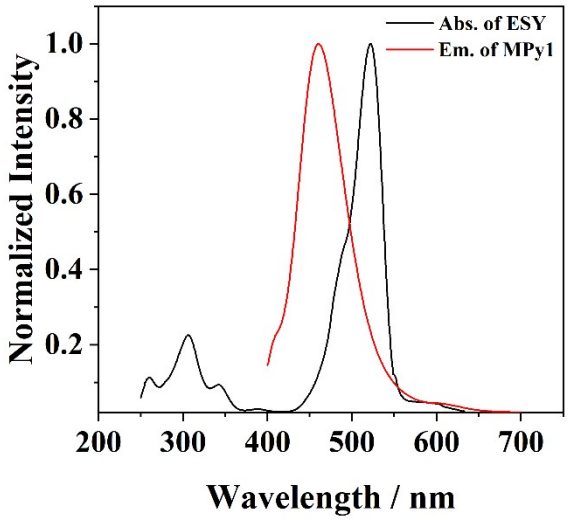

Figure S40. Normalized absorption spectrum of ESY and emission spectrum of **MPy1**.

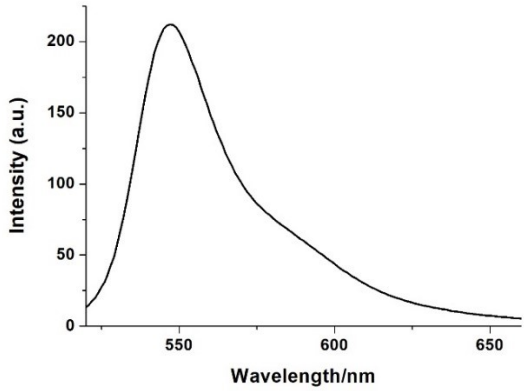

Figure S41. Fluorescence spectra of ESY in H_2O−DMSO (3:2, v/v) (λ_{ex} = 500 nm).

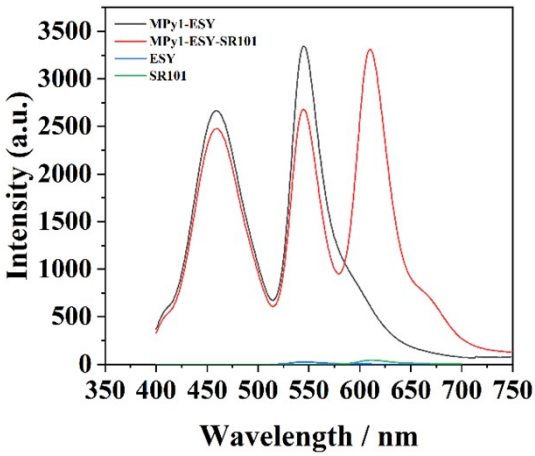

Figure S42. Fluorescence spectra of **MPy1**−ESY, **MPy1**−ESY−SR101, SR101 and ESY (λ_{ex} = 384 nm) in H_2O−DMSO (3:2; v/v).

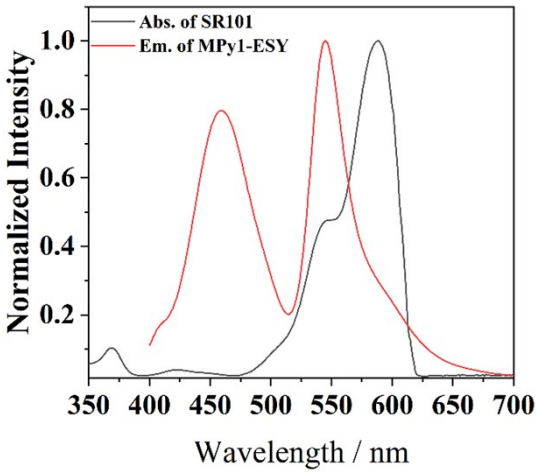

Figure S43. Normalized absorption spectrum of SR101 and emission spectrum of **MPy1**−ESY assembly.

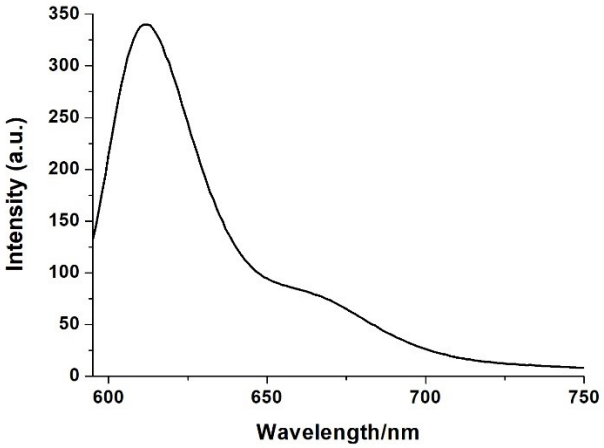

Figure S44. Fluorescence spectra of SR101 in H_2O−DMSO (3:2, v/v) (λ_{ex} = 580 nm).

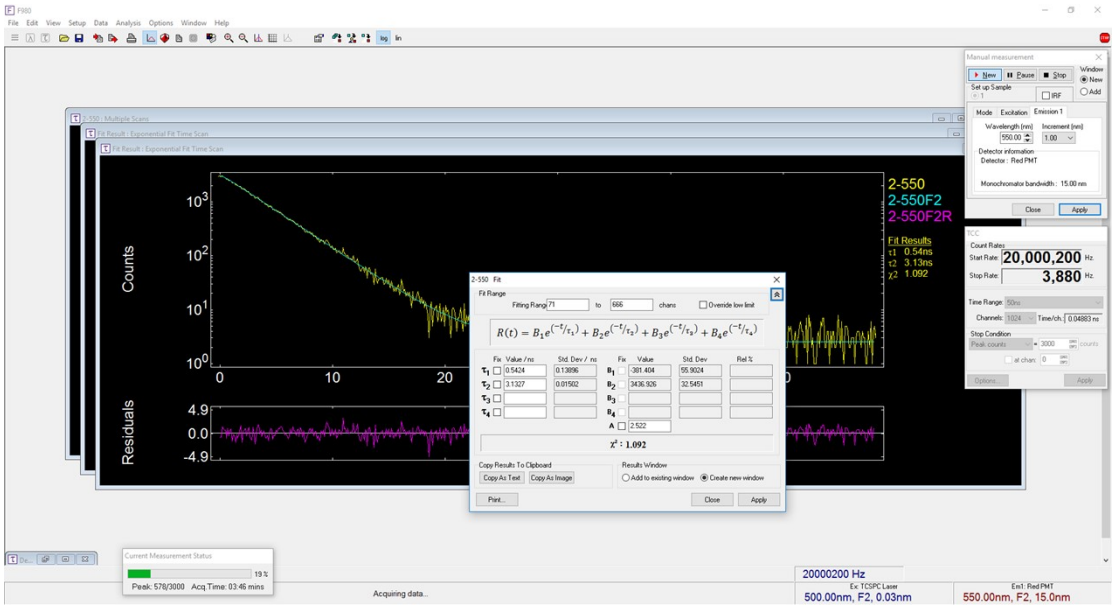

Figure S45. Fluorescence decay profile of ESY in H_2O−DMSO (3:2, v/v) monitored at 550 nm.

Figure S46. Fluorescence decay profile of SR101 in H_2O−DMSO (3:2, v/v) monitored at 612 nm.

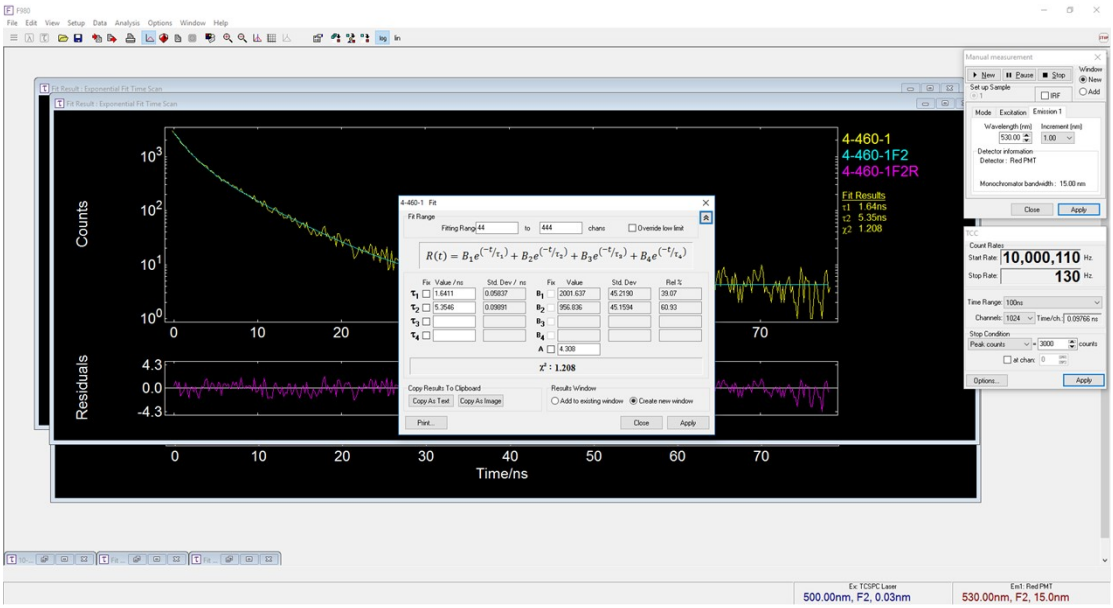

Figure S47. Fluorescence decay profile of **MPy1** assembly in H_2O−DMSO (3:2; v/v) monitored at 460 nm upon excitation at 375 nm.

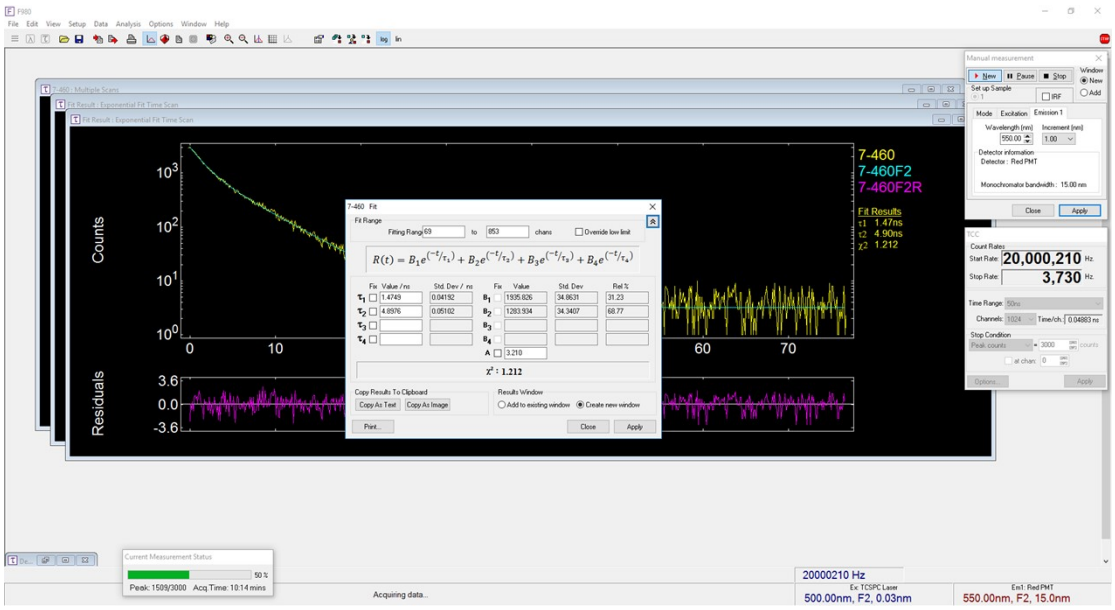

Figure S48. Fluorescence decay profile of **MPy1**−ESY (300:1) assembly in H_2O−DMSO (3:2; v/v) monitored at 460 nm upon excitation at 375 nm.

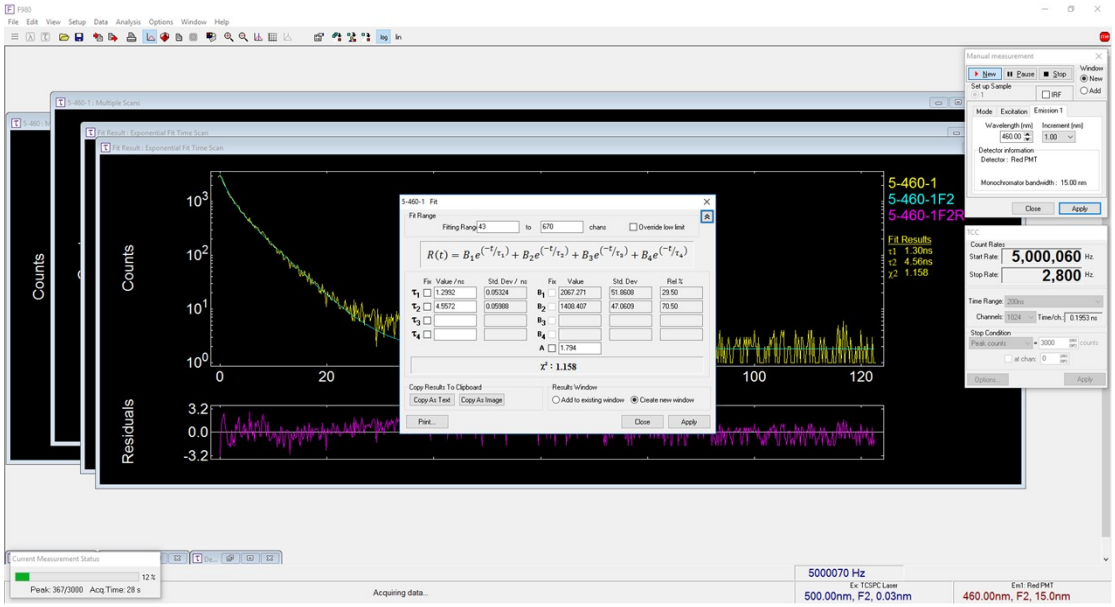

Figure S49. Fluorescence decay profile of **MPy1**−ESY (100:1) assembly in H_2O−DMSO (3:2; v/v) monitored at 460 nm upon excitation at 375 nm.

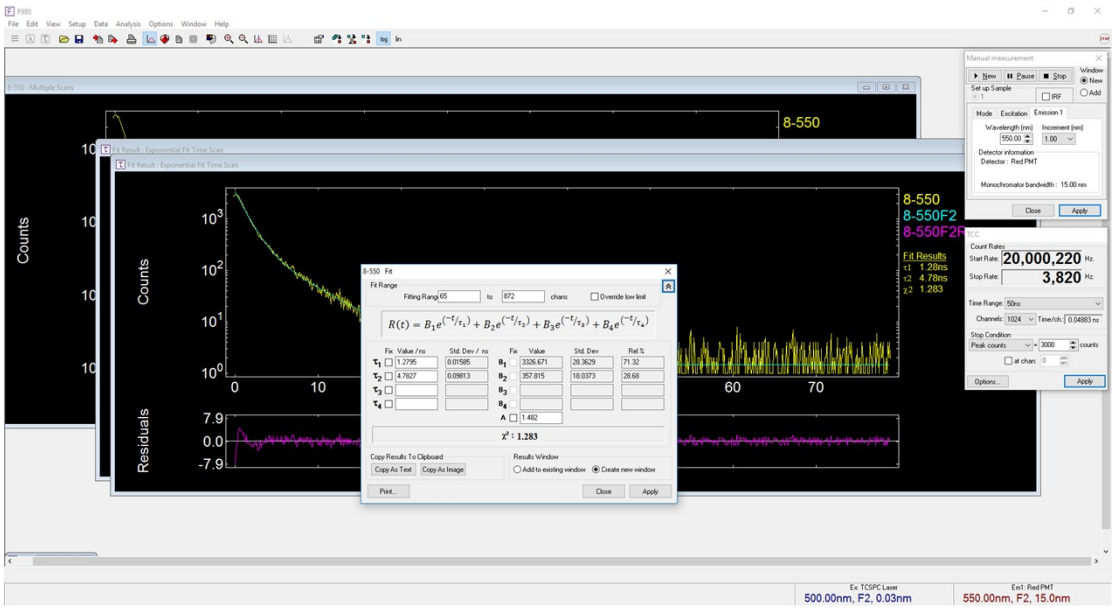

Figure S50. Fluorescence decay profile of **MPy1**−ESY (100:1) assembly monitored at 550 nm upon excitation at 375 nm.

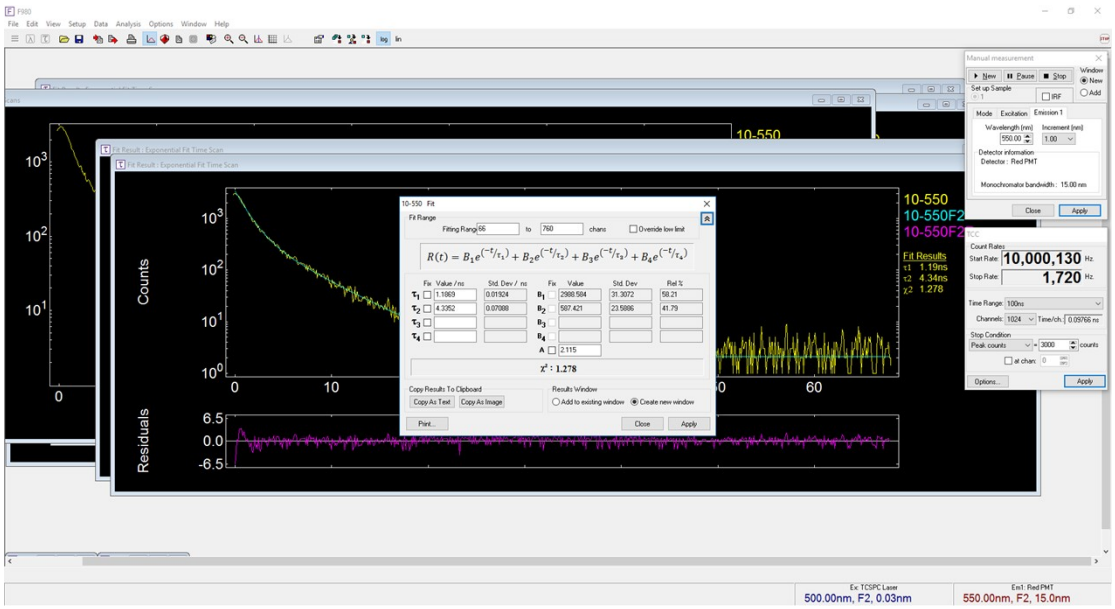

Figure S51. Fluorescence decay profile of **MPy1**−ESY−SR101 (200:2:0.5) assembly monitored at 550 nm upon excitation at 375 nm.

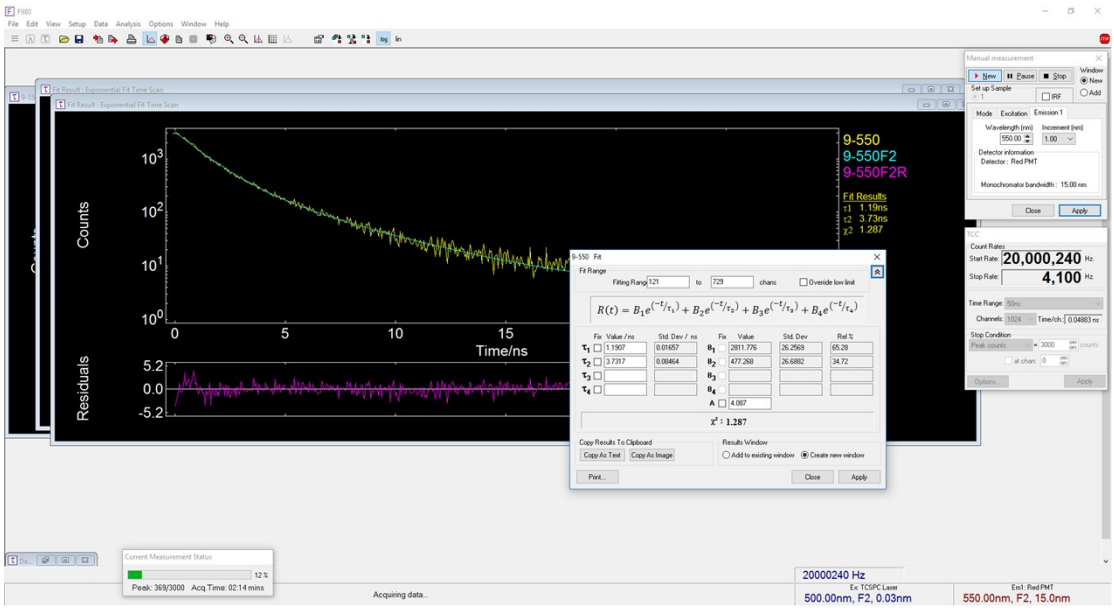

Figure S52. Fluorescence decay profile of **MPy1**−ESY−SR101 (200:2:1) assembly monitored at 550 nm upon excitation at 375 nm.

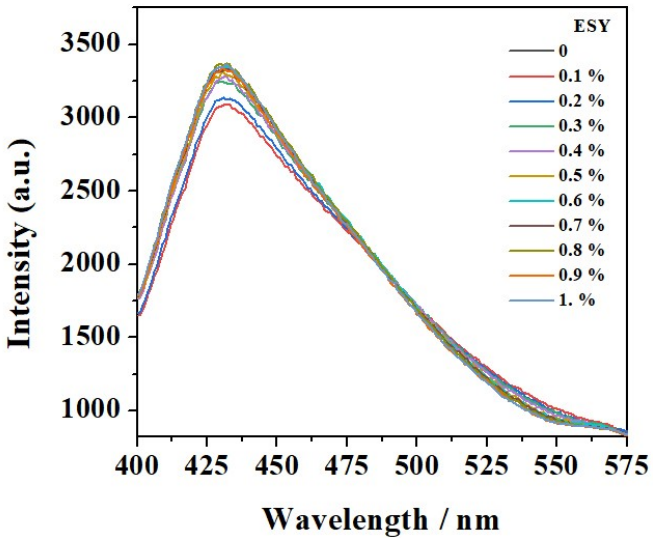

Figure S53. Fluorescence spectra of **MPy3** with different concentrations of ESY in H_2O−DMSO (3:2; v/v).

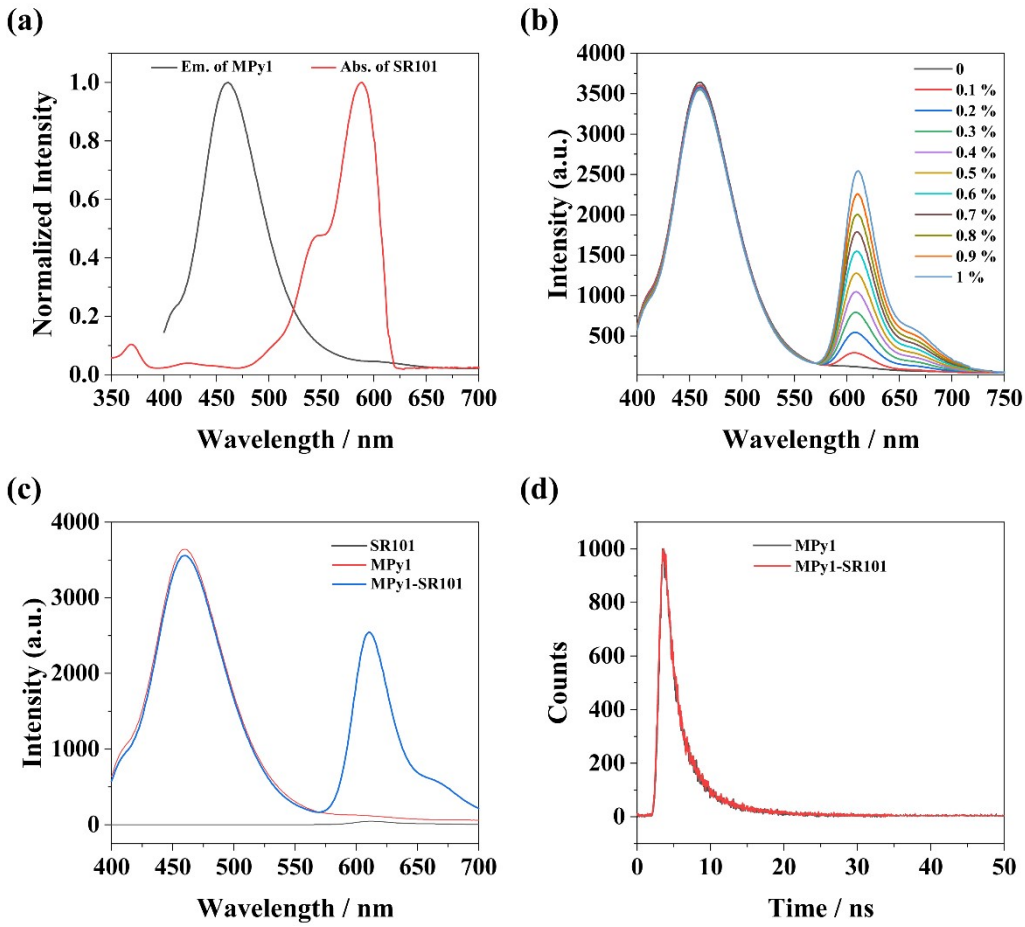

Figure S54. (a) Normalized absorption spectrum of SR101 and emission spectrum of **MPy1**. (b) Fluorescence spectra of **MPy1** with different concentrations of SR101 (λ_{ex} = 384 nm) in H_2O−DMSO (3:2; v/v). (c) Fluorescence spectra of **MPy1**, **MPy1**−SR101, SR101 (λ_{ex} = 384 nm) in H_2O−DMSO (3:2; v/v). (d) Fluorescence decay profiles of **MPy1** nanoparticles (black line) and **MPy1**−SR101 nanoparticles (**MPy1**:SR101 = 100:1) in H_2O−DMSO (3:2; v/v).

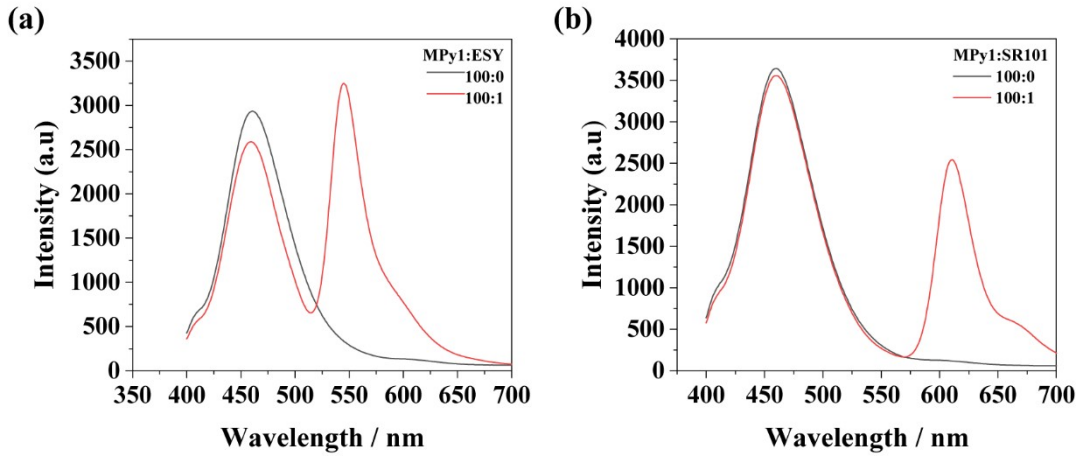

Figure S55. Fluorescence spectra of (a) **MPy1** and **MPy1**−ESY assembly and (b) **MPy1** and **MPy1**−SR101 assembly. [**MPy1**] = 1.0 × 10^{-5} M.

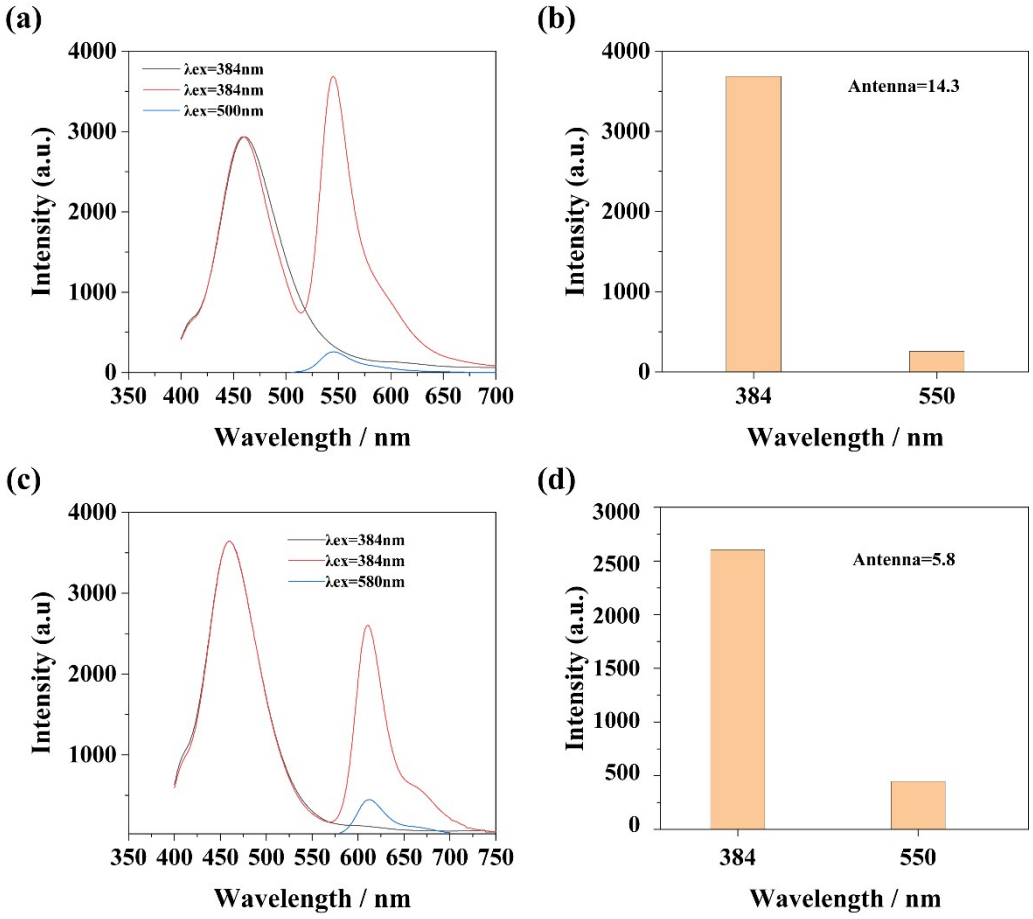

Figure S56. (a) Fluorescence spectra of **MPy1**−ESY (black line, [**MPy1**] = 1.0×10^{-5} M, [ESY] = 1.0×10^{-7} M, λ_{ex} = 384 nm), the donor (red line, λ_{ex} = 384 nm) and

acceptor (blue line, λ_{ex} = 500 nm). The fluorescence intensity of **MPy1**−ESY at 460 nm was normalized according to the fluorescence intensity of the donor; (b) The histogram of the emission intensity of **MPy1**−ESY at 550 nm on the excitation of the donor (λ_{ex} = 384 nm) and acceptor (λ_{ex} = 500 nm). (c) Fluorescence spectra of **MPy1**−SR101 (black line, [**MPy1**] = 1.0×10^{-5} M, [SR101] = 1.0×10^{-7} M, λ_{ex} = 384 nm), the donor (red line, λ_{ex} = 384 nm) and the acceptor (blue line, λ_{ex} = 580 nm). The fluorescence spectrum of **MPy1**−SR101 was normalized according to the fluorescence intensity at 460 nm; (d) The histogram of the emission intensity of **MPy1**−SR101 at 610 nm on the excitation of the donor (λ_{ex} = 384 nm) and acceptor (λ_{ex} = 580 nm).

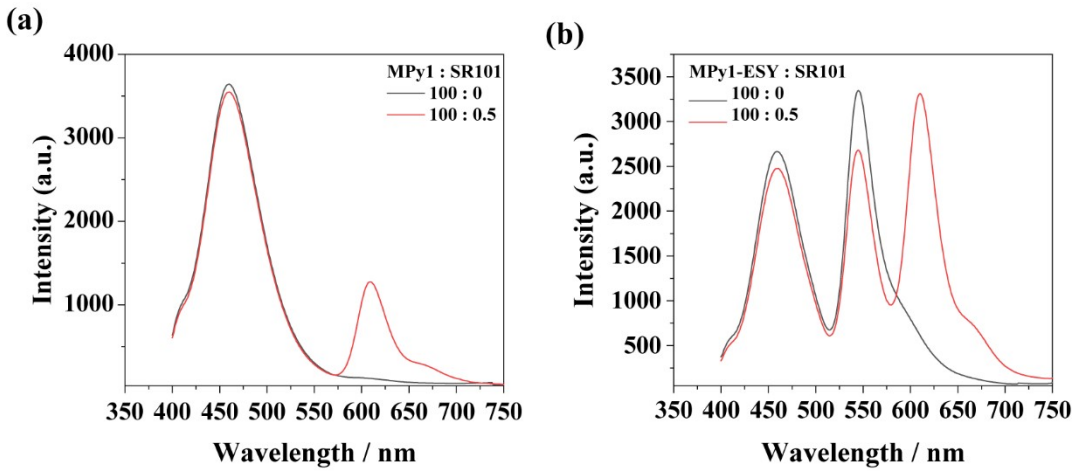

Figure S57. Fluorescence spectra of a) **MPy1** and **MPy1**−SR101 assembly, b) **MPy1**−**ESY** and **MPy1**−ESY−SR101 assembly. [**MPy1**] = 1.0×10^{-5}M.

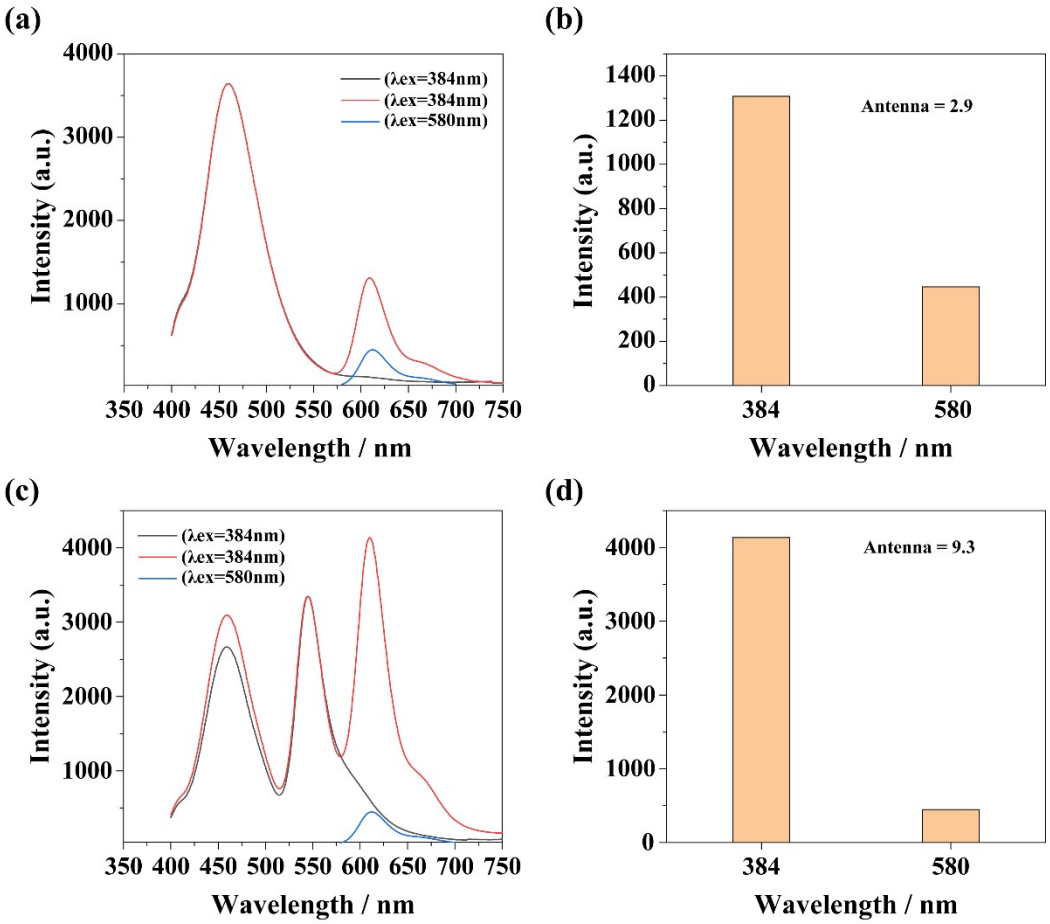

Figure S58. (a) Fluorescence spectra of **MPy1**−SR101 (black line, [**MPy1**] = 1.0×10^{-5} M, [SR101] = 5.0×10^{-8} M, λ_{ex} = 384 nm), the donor (red line, λ_{ex} = 384 nm) and acceptor (blue line, λ_{ex} = 580 nm). The fluorescence intensity of **MPy1**−SR101 at 460 nm was normalized according to the fluorescence intensity of the donor; (b) The histogram of the emission intensity of **MPy1**-SR101 at 610 nm on the excitation of the donor (λ_{ex} = 384 nm) and acceptor (λ_{ex} = 580 nm). (c) Fluorescence spectra of **MPy1**−ESY−SR101 (black line, [**MPy1**] = 1.0×10^{-5} M, [ESY] = 1.0×10^{-7} M, [SR101] = 5.0×10^{-8} M, λ_{ex} = 384 nm), the donor (red line, λ_{ex} = 384 nm) and the acceptor (blue line, λ_{ex} = 580 nm). The fluorescence spectrum of **MPy1**−ESY−SR101 was normalized according to the fluorescence intensity at 550 nm; (d) The histogram of the emission intensity of **MPy1**−ESY−SR101 at 610 nm on the excitation of the donor (λ_{ex} = 384 nm) and acceptor (λ_{ex} = 580 nm).

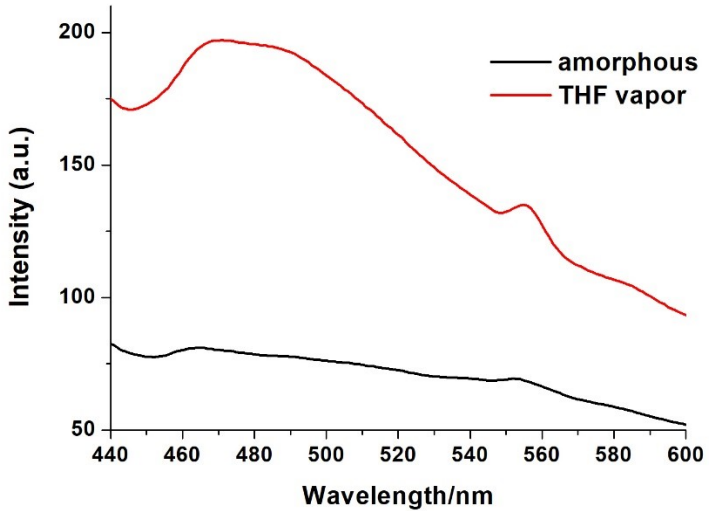

Figure S59. Fluorescence spectra of **MPy1** in different solid states: amorphous and fuming with THF vapor for 5 min (λ_{ex} = 384 nm).

9. References

[1] Zhang, D.; Li, D.; Li, X.; Jin, W. Post-Assembly Polymerization of Discrete Organoplatinum(II) Metallacycles via Dimerization of Coumarin Pendants. *Dyes Pigm*. **2018**, *152*, 43−48.

[2] Ghosh, K.; Yang, H.; Northrop, B.; Lyndon, M. M.; Zheng, Y.; Muddiman, D. C.; Stang, P. J. Coordination-Driven Self-Assembly of Cavity-Cored Multiple Crown Ether Derivatives and Poly[2]pseudorotaxanes. *J. Am. Chem. Soc.* **2008**, *130*, 5320−5334.

[3] Ferrando-Soria, J.; Fernandez, A.; Vitorica-Yrezabal, I. J.; Asthana, D.; Muryn, C. A.; Tuna, F.; Timco, G. A.; Winpenny. R. E. P. Formation of an Interlocked Double-Chain from an Organic–Inorganic [2]rotaxane. *Chem. Commun.* **2019**, *55*, 2960−2963.